Essential role of the cytochrome P450 CYP4F22 in the production of acylceramide, the key lipid for skin permeability barrier formation

Yusuke Ohno[a], Shota Nakamichi[a], Aya Ohkuni[a], Nozomi Kamiyama[a], Ayano Naoe[b], Hisashi Tsujimura[b], Urara Yokose[b], Kazumitsu Sugiura[c], Junko Ishikawa[b], Masashi Akiyama[c], and Akio Kihara[a,1]

[a]Laboratory of Biochemistry, Faculty of Pharmaceutical Sciences, Hokkaido University, Kita-ku, Sapporo 060-0812, Japan; [b]Kao Corporation, Haga-gun, Tochigi 321-3497, Japan; and [c]Department of Dermatology, Nagoya University Graduate School of Medicine, Showa-ku, Nagoya 466-8550, Japan

Edited by David W. Russell, University of Texas Southwestern Medical Center, Dallas, TX, and approved May 21, 2015 (received for review February 19, 2015)

A skin permeability barrier is essential for terrestrial animals, and its impairment causes several cutaneous disorders such as ichthyosis and atopic dermatitis. Although acylceramide is an important lipid for the skin permeability barrier, details of its production have yet to be determined, leaving the molecular mechanism of skin permeability barrier formation unclear. Here we identified the cytochrome P450 gene *CYP4F22* (cytochrome P450, family 4, subfamily F, polypeptide 22) as the long-sought fatty acid ω-hydroxylase gene required for acylceramide production. *CYP4F22* has been identified as one of the autosomal recessive congenital ichthyosis-causative genes. Ichthyosis-mutant proteins exhibited reduced enzyme activity, indicating correlation between activity and pathology. Furthermore, lipid analysis of a patient with ichthyosis showed a drastic decrease in acylceramide production. We determined that CYP4F22 was a type I membrane protein that locates in the endoplasmic reticulum (ER), suggesting that the ω-hydroxylation occurs on the cytoplasmic side of the ER. The preferred substrate of the CYP4F22 was fatty acids with a carbon chain length of 28 or more (≥C28). In conclusion, our findings demonstrate that CYP4F22 is an ultra-long-chain fatty acid ω-hydroxylase responsible for acylceramide production and provide important insights into the molecular mechanisms of skin permeability barrier formation. Furthermore, based on the results obtained here, we proposed a detailed reaction series for acylceramide production.

acylceramide | ceramide | lipid | skin | sphingolipid

A skin permeability barrier protects terrestrial animals from water loss from inside the body, penetration of external soluble materials, and infection by pathogenetic organisms. In the stratum corneum, the outermost cell layer of the epidermis, multiple lipid layers (lipid lamellae) play a pivotal function in barrier formation (Fig. S1) (1–3). Impairment of the skin permeability barrier leads to several cutaneous disorders, such as ichthyosis, atopic dermatitis, and infectious diseases.

The major components of the lipid lamellae are ceramide (the sphingolipid backbone), cholesterol, and free fatty acid (FA). In most tissues, ceramide consists of a long-chain base (LCB; usually sphingosine) and an amide-linked FA with a chain length of 16–24 (C16–C24) (4, 5). On the other hand, ceramide species in the epidermis are strikingly unique (Fig. S2*A*). For example, epidermal ceramides contain specialized LCBs (phytosphingosine and 6-hydroxysphingosine) and/or FAs with α- or ω-hydroxylation (1–3). In addition, substantial amounts of epidermal ceramides have ultra-long-chain FAs (ULCFAs) with chain lengths of 26 or more (≥C26) (4, 5). Unique epidermal ceramides are acylceramides having C28–C36 ULCFAs, which are ω-hydroxylated and esterified with linoleic acid [EOS in Fig. S1; EODS, EOS, EOP, and EOH in Fig. S2*A*; EOS stands for a combination of an esterified ω-hydroxy FA (EO) and sphingosine (S); DS, dihydrosphingosine; P, phytosphingosine; H, 6-hydroxysphingosine] (1–3, 6, 7). These characteristic molecules may be important to increase the hydrophobicity of lipid lamellae and/or to stabilize the multiple lipid layers. Linoleic acid is one of the essential FAs, and its deficiency causes ichthyosis symptoms resulting from a failure to form normal acylceramide (8). Ichthyosis is a cutaneous disorder accompanied by dry, thickened, and scaly skin; it is caused by a barrier abnormality. In patients who have atopic dermatitis, both total ceramide levels and the chain length of ceramides are decreased, and ceramide composition is altered also (9–11).

In addition to its essential function in the formation of lipid lamellae, acylceramide also is important as a precursor of protein-bound ceramide, which functions to connect lipid lamellae and corneocytes (Fig. S1) (12, 13). After the removal of linoleic acid, the exposed ω-hydroxyl group of acylceramide is covalently bound to corneocyte proteins, forming a corneocyte lipid envelope. Acylceramides and protein-bound ceramides are important in epidermal barrier formation, and mutations in the genes involved in their synthesis, including the ceramide synthase *CERS3*, the 12(*R*)-lipoxygenase *ALOX12B*, and the epidermal lipoxygenase-3 *ALOXE3*, can cause nonsyndromic, autosomal recessive congenital ichthyosis (ARCI) (3, 14–16). CERS3 catalyzes the amide bond formation between an LCB and ULCFA, producing ULC-ceramide, which is the precursor of acylceramide (Fig. S1 and Fig. S2*B*) (17). ALOX12B and ALOXE3 are required for the formation of protein-bound ceramides (13, 18). Other ARCI genes include the ATP-binding cassette (ABC) transporter *ABCA12*, the transglutaminase *TGM1*, *NIPAL4* (NIPA-like domain containing

Significance

The sphingolipid backbone ceramide is the major lipid species in the stratum corneum and plays a pivotal function in skin permeability barrier formation. Acylceramide is an important epidermis-specific ceramide species. However, the details of acylceramide production, including its synthetic genes, reactions and their orders, and intracellular site for production, have remained unclear. In the present study, we identified the cytochrome P450, family 4, subfamily F, polypeptide 22 (CYP4F22) as the missing fatty acid ω-hydroxylase required for acylceramide synthesis. We also determined that CYP4F22 is a type I endoplasmic reticulum membrane protein and that its substrate is ultra-long-chain fatty acids. Our findings provide important insights into the molecular mechanisms of not only acylceramide production but also skin permeability barrier formation.

Author contributions: A.K. planned the project; Y.O. and A.K. designed research; K.S. and M.A. prepared stratum corneum samples; Y.O., S.N., A.O., and N.K. performed research; A.N., H.T., U.Y., and J.I. analyzed ceramide compositions; Y.O. analyzed data; and A.K. wrote the paper.

The authors declare no conflict of interest.

This article is a PNAS Direct Submission.

[1]To whom correspondence should be addressed. Email: kihara@pharm.hokudai.ac.jp.

This article contains supporting information online at www.pnas.org/lookup/suppl/doi:10.1073/pnas.1503491112/-/DCSupplemental.

4)/*ICHTHYIN*, *CYP4F22/FLJ39501*, *LIPN* (lipase, family member N), and *PNPLA1* (patatin-like phospholipase domain containing 1) (16, 19). The exact functions of *NIPAL4*, *LIPN*, and *PNPLA1* are currently unclear. Causative genes of syndromic forms of ichthyosis also include a gene required for acylceramide synthesis: the FA elongase *ELOVL4*, which produces ULCFA-CoAs, the substrate of CERS3 (20).

Although acylceramide is essential for the epidermal barrier function, the mechanism behind acylceramide production is still poorly understood, leaving the molecular mechanisms behind epidermal barrier formation unclear. For example, acylceramide production requires ω-hydroxylation of the FA moiety of ceramide. However, the ω-hydroxylase responsible for this reaction was unidentified heretofore (Fig. S1). Here, we identified the cytochrome P450, family 4, subfamily F, polypeptide 22 (CYP4F22), also known as "FLJ39501," as this missing FA ω-hydroxylase required for acylceramide production. *CYP4F22* had been identified as one of the ARCI genes (21), although its function in epidermal barrier formation remained unsolved. Our findings clearly demonstrate a relationship between ARCI pathology, acylceramide levels, and ω-hydroxylase activity.

Results

Identification of CYP4F22 as the FA ω-Hydroxylase Required for ω-Hydroxyceramide Production. Although researchers have long known that ω-hydroxylation is essential for acylceramide formation, they have puzzled over which gene is responsible for this reaction. To identify this gene, we first established a cell system that produced ULC-ceramides, a possible substrate of interest for ω-hydroxylase, because most cells cannot produce such extremely long ceramides. HEK 293T cells overproducing the FA elongase ELOVL4 and/or the ceramide synthase CERS3 were labeled with [^{3}H]sphingosine, and the chain lengths of ceramides were determined by reverse-phase TLC. Although overexpression of either ELOVL4 or CERS3 alone did not result in the production of ULC-ceramides, their co-overproduction caused generation of ULC-ceramides with ≥C26 (Fig. 1*A*). They migrated more slowly than long-chain (LC; C16–C20) ceramides and very long-chain (VLC; C22–C24) ceramides on reverse-phase TLC. Production of ULC-ceramides with chain lengths up to C36 also was confirmed by LC-MS analysis (Fig. S3). When labeled lipids were separated by normal-phase TLC, ULC-ceramides were detected as a band at the adjacent, upper position of VLC-ceramides (Fig. 1*B*).

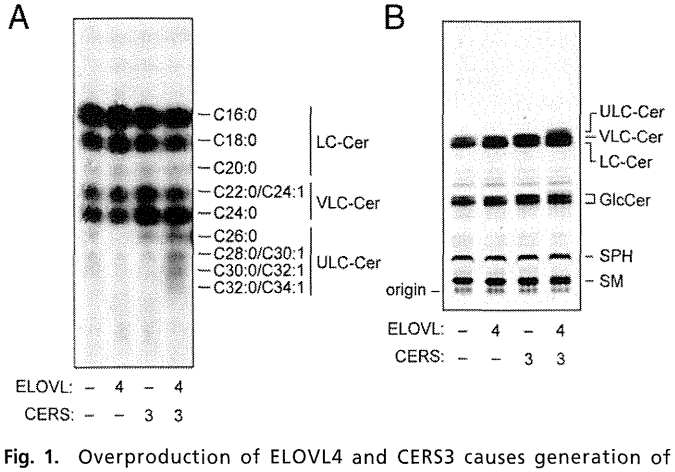

Fig. 1. Overproduction of ELOVL4 and CERS3 causes generation of ULC-ceramides. HEK 293T cells were transfected with plasmids encoding *3xFLAG-ELOVL4* and *3xFLAG-CERS3*, as indicated. Cells were labeled with [^{3}H]sphingosine for 4 h at 37 °C. Lipids were extracted, separated by reverse-phase TLC (*A*) or normal-phase TLC (*B*), and detected by autoradiography. Cer, ceramide; GlcCer, glucosylceramide; SM, sphingomyelin; SPH, sphingosine.

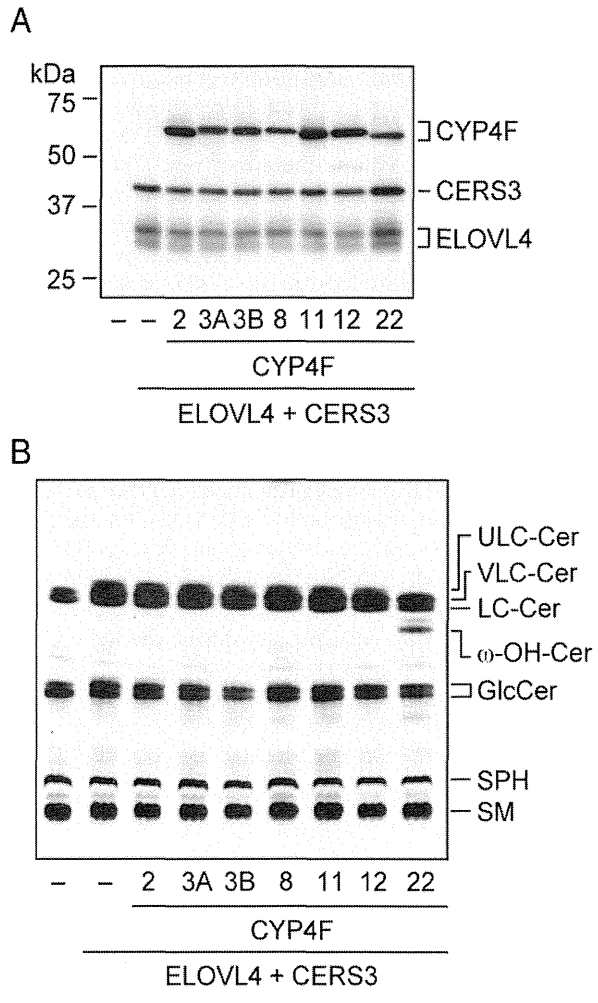

Fig. 2. CYP4F22 is involved in ω-hydroxyceramide synthesis. HEK 293T cells were transfected with plasmids encoding *3xFLAG-ELOVL4*, *3xFLAG-CERS3*, and *3xFLAG-CYP4F* subfamily members, as indicated. (*A*) Total lysates prepared from the transfected cells were separated by SDS/PAGE, followed by immunoblotting with anti-FLAG antibodies. (*B*) Cells were labeled with [^{3}H]sphingosine for 4 h at 37 °C. Lipids were extracted, separated by normal-phase TLC, and detected by autoradiography. Cer, ceramide; GlcCer, glucosylceramide; SM, sphingomyelin; SPH, sphingosine; ω-OH, ω-hydroxy.

It has been reported that the cytochrome P450 (CYP) inhibitor aminobenzotriazole inhibits the generation of ω-hydroxyceramide in cultured human keratinocytes (22). In humans, 57 *CYP* genes exist, and mammalian *CYP* genes are classified into 18 families and 43 subfamilies. Some CYP4F members are implicated in the ω-hydroxylation of long-chain FAs (23, 24), raising the possibility that certain CYP4F subfamily members are responsible for ω-hydroxylation of ULCFAs in acylceramide formation. To test this possibility, we cloned all the human *CYP4F* subfamily genes (*CYP4F2*, *3A*, *3B*, *8*, *11*, *12*, and *22*), and each was expressed as an N-terminally 3xFLAG-tagged protein in HEK 293T cells overproducing 3xFLAG-ELOVL4 and 3xFLAG-CERS3. All CYP4F subfamily proteins were expressed at similar levels (Fig. 2*A*). Among the CYP4F subfamily members, only CYP4F22 caused the disappearance of ULC-ceramide, which was concomitant with the production of a new band at the position of ω-hydroxyceramide (Fig. 2*B* and Fig. S4). LC-MS analysis determined that this band indeed represented ω-hydroxyceramides with C28–C36 (Fig. S5). Thus, CYP4F22 is the ω-hydroxylase required for ω-hydroxyceramide production.

Correlation Between CYP4F22 Activity and Ichthyosis Pathology. Although the *CYP4F22* gene has been identified as one of the

ARCI-causative genes (21, 25), its function in epidermal barrier formation has remained unsolved. Five missense mutations, all of which cause amino acid substitutions (F59L, R243H, R372W, H435Y, and H436D), have been found in the *CYP4F22* of patients with ichthyosis. To examine their role in ichthyosis pathology, we introduced these mutations into *CYP4F22* and examined the ω-hydroxylase activity of the resultant mutant proteins. All mutant proteins were expressed at levels equivalent to the wild-type protein (Fig. 3*A*), and indeed all ω-hydroxylase activity of the mutant CYP4F22 proteins decreased to 4–20% of wild-type protein activity (Fig. 3*B*). Therefore, protein activity and ichthyosis pathology were nicely correlated.

Those points being noted, ichthyosis resulting from *CYP4F22* mutation is quite rare. In fact, only ~20 patients have been reported in Mediterranean populations (21), and only a single patient has been reported in Japan (25). The Japanese patient has compound heterozygous *CYP4F22* mutations: One is a point mutation (c.728G→A) causing an amino acid substitution (p.R243H; R243H), and the other is a deletion (c.1138delG) causing a frame shift (p.D380TfsX2; D380TfsX2) in which Asp380 is replaced by Thr followed by a stop codon (25). The mutant R243H exhibited decreased activity as described above (Fig. 3*B*). We also introduced the c.1138delG mutation into *CYP4F22* and examined the ω-hydroxylase activity of its truncated protein product. D380TfsX2 (predicted molecular mass, 44.8 kDa) migrated faster than the wild-type protein (62.0 kDa; Fig. 3*A*), and we found that it exhibited no activity (Fig. 3*B*).

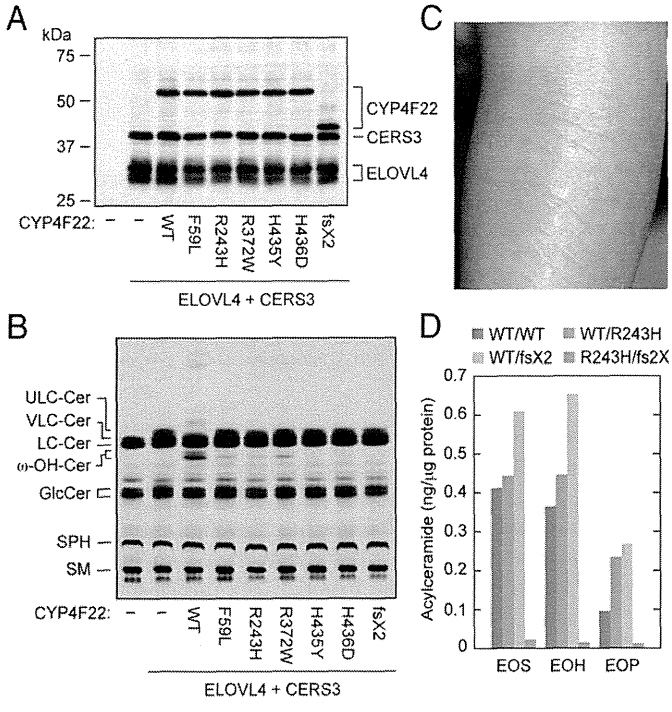

Fig. 3. Hydroxylase activity of CYP4F22 is impaired by ichthyosis-causing mutations. (*A* and *B*) HEK 293T cells were transfected with plasmids encoding *3xFLAG-ELOVL4*, *3xFLAG-CERS3*, and *3xFLAG-CYP4F22* (wild type or mutant), as indicated. (*A*) Total cell lysates prepared from the transfected cells were separated by SDS/PAGE and subjected to immunoblotting with anti-FLAG antibodies. (*B*) The transfected cells were labeled with [^{3}H]sphingosine for 4 h at 37 °C. Extracted lipids were separated by normal-phase TLC and detected by autoradiography. Cer, ceramide; GlcCer, glucosylceramide; SM, sphingomyelin; SPH, sphingosine; ω-OH, ω-hydroxy. (*C*) Representative clinical feature of a 2-y-old ARCI patient. Leaf-like flakes presented on the extensor side of the left lower limb before tape stripping. (*D*) Acylceramide (EOS, EOH, and EOP) levels in stratum corneum of a control (WT/WT), carriers (WT/R243H, the ichthyosis patient's father, and WT/D380T fs2X (fs2X), the patient's mother), and an ARCI patient (R243H/D380T fs2X) were measured by LC-MS.

To confirm our conclusion that CYP4F22 is involved in the production of acylceramide through ω-hydroxyceramide synthesis, we subjected the stratum corneum of the Japanese patient (Fig. 3*C*) and those of controls (her parents and a healthy volunteer) to LC-MS analysis and examined the levels of 11 major ceramide species. Although statistical analysis could not be performed because of the low number of samples, all three acylceramides containing sphingosine (EOS), 6-hydroxysphingsoine (EOH), and phytosphingosine (EOP) were apparently decreased in the ARCI patient to one tenth of the levels in controls (Fig. 3*D* and Table S1). Instead, the nonacylated ceramides NS (which is a combination of sphingosine and a nonhydroxylated FA) and AS (which is a combination of sphingosine and an α-hydroxylated FA) seemed to be increased (Table S1). These results confirm that ω-hydroxyceramide production by CYP4F22 is indeed required for acylceramide synthesis.

CYP4F22 Is a Type I Endoplasmic Reticulum Membrane Protein. We next examined the subcellular localization of CYP4F22 by subjecting 3xFLAG-tagged CYP4F22 to indirect immunofluorescence microscopy (Fig. 4*A*). 3xFLAG-CYP4F22 exhibited a reticular localization pattern and was colocalized with calnexin, HA-ELOVL4, and HA-CERS3, all of which are endoplasmic reticulum (ER) proteins, indicating that CYP4F22 is localized in the ER. A hydropathy plot showed that CYP4F22 contains a highly hydrophobic region at the N terminus as well as some weak hydrophobic stretches (Fig. 4*B*). To reveal the membrane topology of CYP4F22, we introduced an N-glycosylation cassette, which is N-glycosylated when exposed to the lumen of the ER, into several positions of CYP4F22: the N terminus, E85/K (between Glu85 and Lys86 residues), H155/R, A285/L, C361/R, D455/N, and R508/K. Of these fusion proteins, only CYP4F22 containing the N-glycosylation cassette at the N terminus received glycosylation, because the shift in molecular weight was observed upon treatment with endoglycosidase H (Fig. 4*C*). This result indicates that CYP4F22 spans the ER membrane once. Furthermore, it oriented its N terminus to the ER lumen and oriented the large, hydrophilic C-terminal domain containing the active site to the cytosolic side of the ER membrane. The same membrane topology was determined for other CYP members by the detection of N-terminal N-glycosylation (26, 27).

When the N-terminal hydrophobic region was removed, the resulting CYP4F22ΔN became distributed throughout the cytoplasm (Fig. 4*D*). CYP4F22ΔN was fractionated into both soluble and membrane fractions by ultracentrifugation, in contrast to full-length CYP4F22, which was detected only in the membrane fraction (Fig. 4*E*). These results confirmed that CYP4F22 is a type I ER membrane protein. CYP4F22ΔN could not produce ω-hydroxyceramide (Fig. 4*F*), suggesting that anchoring to the ER membrane, where all the reactions of acylceramide synthesis occur, is crucial for the CYP4F22 function.

ULCFAs Are Substrates of CYP4F22. It was still unclear whether CYP4F22 introduces an ω-hydroxyl group into ULCFAs before or after the formation of ceramide. Therefore, we examined ω-hydroxy FA levels using LC-MS in the presence of the ceramide synthase inhibitor fumonisin B_1. If ω-hydroxylation occurs before ceramide production, it was expected that free ω-hydroxy FA levels should be increased with fumonisin B_1 treatment. We found that ω-hydroxy FA levels with C26–C36 were increased significantly by the addition of fumonisin B_1 (Fig. 5*A*), suggesting that ω-hydroxylation occurs before ceramide production. Thus, it is highly likely that the substrates of CYP4F22 are not ceramides but rather are FAs, the same type of substrate catalyzed by other CYP4F family members.

To confirm that the substrates of CYP4F22 are FAs, we performed an in vitro analysis using yeast, which has no endogenous FA ω-hydroxylase activity. When C30:0 FA was used as a substrate,

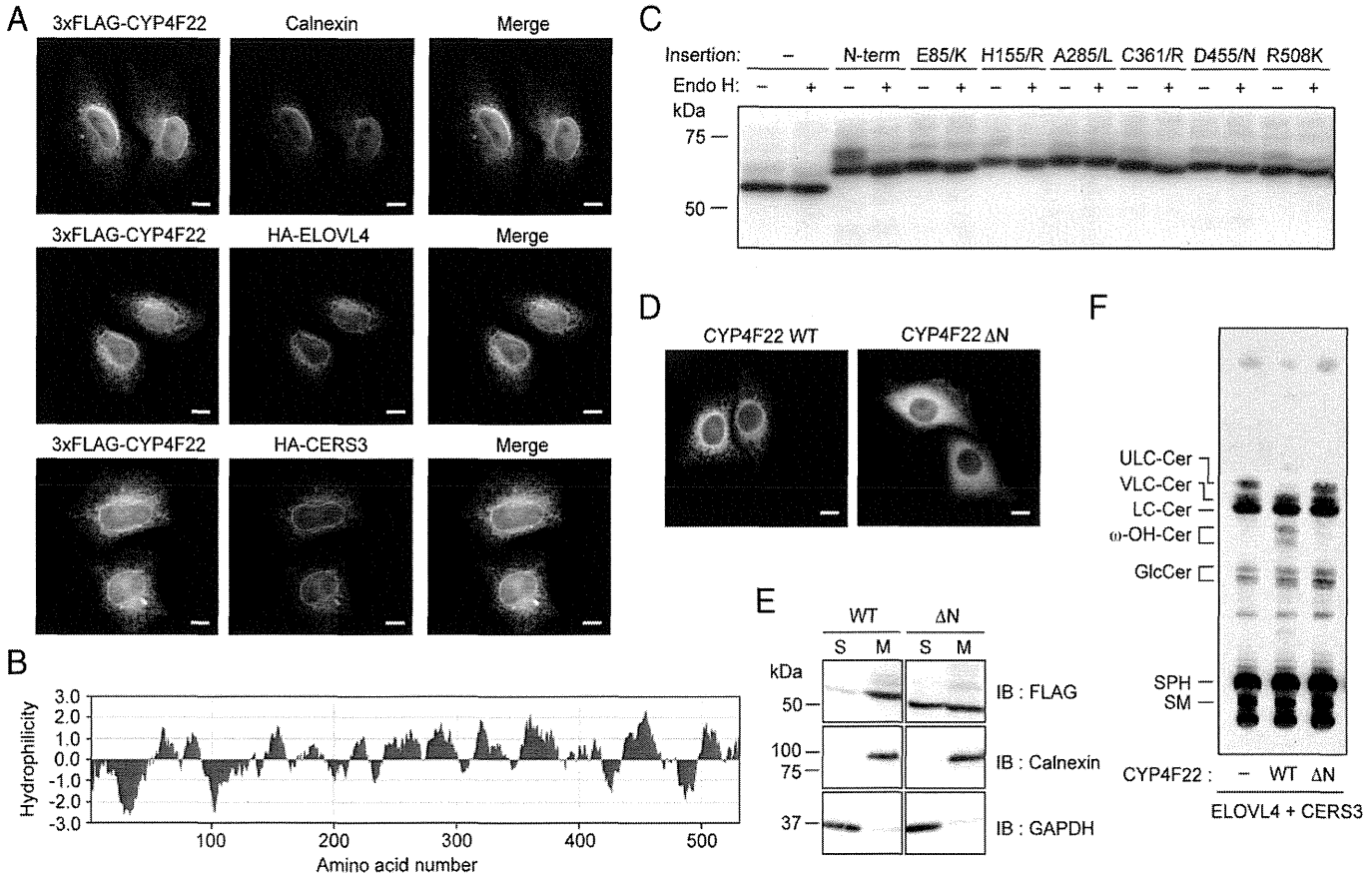

Fig. 4. CYP4F22 is a type I ER membrane protein. (*A*, *D*, and *E*) HeLa cells were transfected with plasmids encoding *HA-ELOVL4*, *HA-CERS3*, *3xFLAG-CYP4F22*, and *3xFLAG-CYP4F22ΔN* (CYP4F22 lacking 54 N-terminal amino acids), as indicated. (*A* and *D*) Cells were subjected to indirect immunofluorescence microscopic observation. (Scale bars, 10 μm.) (*B*) The hydrophilicity of CYP4F22 was analyzed by MacVector software (MacVector) using the Kyte and Doolittle algorithm (window size, 15). (*C*) HEK 293T cells were transfected with pCE-puro 3xFLAG-CYP4F22, pCE-puro 3xFLAG-CYP4F22 (N-term: insertion of the N-glycosylation cassette to the N terminus), pCE-puro 3xFLAG-CYP4F22 (E85/K: insertion of the cassette between Glu-85 and Lys-86), pCE-puro 3xFLAG-CYP4F22 (H155/R), pCE-puro 3xFLAG-CYP4F22 (A285/L), pCE-puro 3xFLAG-CYP4F22 (C361/R), pCE-puro 3xFLAG-CYP4F22 (D455/N), or pCE-puro 3xFLAG-CYP4F22 (R508/K). Lysates (3 μg) prepared from transfected cells were treated with or without endoglycosidase H (Endo H) and were separated by SDS/PAGE, followed by immunoblotting with anti-FLAG antibodies. (*E*) Total cell lysates (10 μg) were centrifuged at 100,000 × *g* for 30 min at 4 °C. The resulting supernatant (soluble fraction, S) and pellet (membrane fraction, M) were subjected to immunoblotting using anti-FLAG, anti-calnexin (membrane protein marker) or anti-GAPDH (soluble protein marker) antibodies. IB, immunoblotting. (*F*) HEK 293T cells transfected with plasmids encoding *3xFLAG-ELOVL4*, *3xFLAG-CERS3*, and *3xFLAG-CYP4F22* [wild type or *CYP4F22ΔN* (ΔN)], as indicated, were labeled with [^{3}H]sphingosine for 4 h at 37 °C. Lipids were extracted, separated by normal-phase TLC, and detected by autoradiography. Cer, ceramide; GlcCer, glucosylceramide; SM, sphingomyelin; SPH, sphingosine; ω-OH, ω-hydroxy.

the total membrane fractions prepared from yeast bearing a vector plasmid exhibited FA ω-hydroxylase activity only at background levels (Fig. 5*B*). On the other hand, the ectopic expression of human CYP4F22 resulted in the production of ω-hydroxy FA in an NADPH-dependent manner (Fig. 5*B*). The hydroxylation reactions by CYP generally require O_2 and NADPH. These results indicated that the substrates of CYP4F22 are indeed FAs.

Acylceramide specifically contains ULCFA (mostly C28–C36) as its FA component. It is possible that the substrate preference of CYP4F22 determines the FA chain length of acylceramides. To examine this possibility, we prepared HEK 293T cells producing different sets of ceramides with specific chain lengths by introducing particular combinations of ceramide synthase and FA elongase (ELOVL1 and CERS2, C22–C24 ceramides; ELOVL1 and CERS3, C26 ceramide; and ELOVL4 and CERS3, ≥C26 ceramides) (Fig. 5*C*) (28, 29). Mammals have six ceramide synthases (CERS1–6) and seven FA elongases (ELOVL1–7), and each exhibits characteristic substrate specificity (Fig. S2*B*) (2, 4, 5, 28). When CYP4F22 was expressed in these cells producing different ceramide species, ω-hydroxyceramides were produced in cells producing C26 ceramide (ELOVL1/CERS3 combination) and ≥C26 ceramides (the ELOVL4/CERS3 combination) but not in cells producing C22–C24 ceramides (the ELOVL1/CERS2 combination) (Fig. 5*D*). These results suggest that CYP4F22 can ω-hydroxylate ULCFAs (≥C26) but not VLCFAs (C22 and C24). The levels of ω-hydroxyceramide produced in ELOVL1/CERS3 cells were similar to those in ELOVL4/CERS3 cells, although the levels of nonhydroxyceramide substrates were much higher in ELOVL1/CERS3 cells (Fig. 5*C*). Thus, CYP4F22 exhibits especially high activity toward ULCFAs with ≥C28.

Discussion

Here we identified CYP4F22 as an ULCFA ω-hydroxylase involved in acylceramide production. Acylceramide is quite important for epidermal barrier formation, and impairment of its production (e.g. by *ELOVL4* and *CERS3* mutations) causes ichthyosis (15, 20). *CYP4F22* was first identified as an ARCI-causative gene by Fischer and her coworkers (21). They proposed that CYP4F22 and most other ichthyosis-causative genes are involved in a metabolic pathway producing 12-lipoxygenase products (hepoxilins and trioxilins) from arachidonic acid by analogy to the 5-lipoxygenase pathway creating leukotrienes. In their scenario, arachidonic acid is first converted to 12(*R*)-hydroperoxyeicosatetraenoic acid [12(*R*)-HPETE] by one of the ichthyosis gene products, ALOX12B, and then to 12(*R*)-hepoxilin A_3 by another ichthyosis gene product, ALOXE3. 12(*R*)-Hepoxilin A_3 is further converted to a triol compound, 12(*R*)-trioxilin A_3. CYP4F22 was proposed to be involved in the metabolism of 12(*R*)-trioxilin A_3 by converting 12(*R*)-trioxilin A_3 to 20-hydroxy-

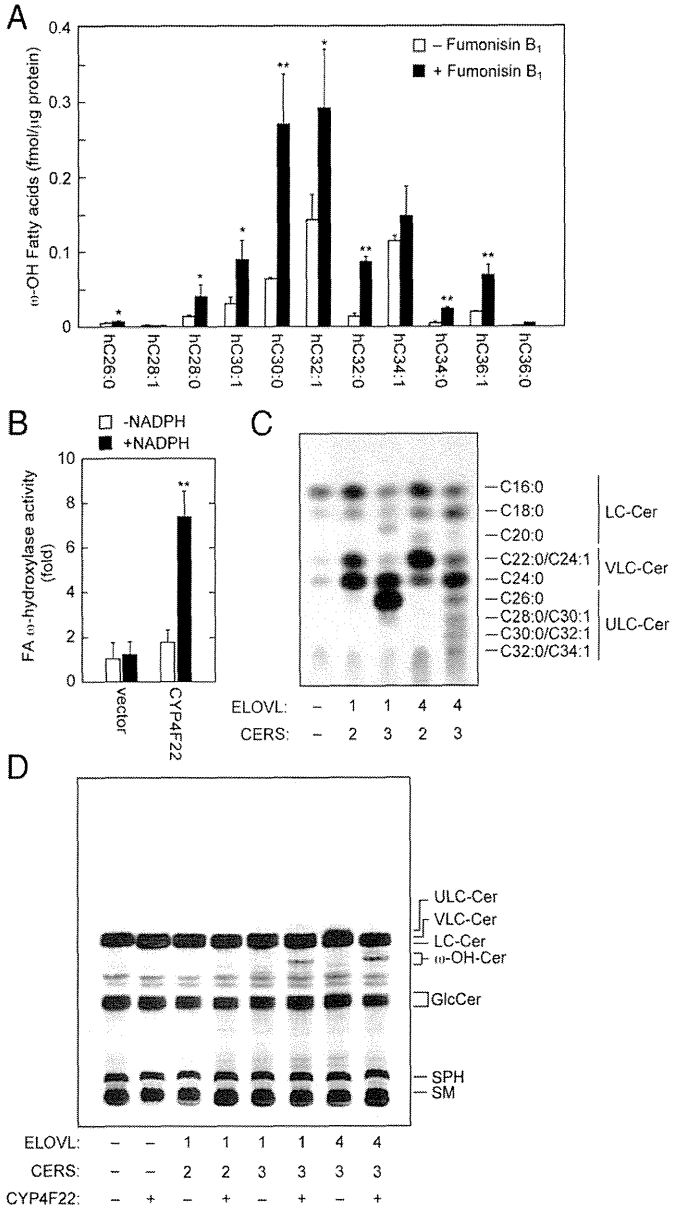

Fig. 5. CYP4F22 hydroxylates ULCFAs. (*A*) Keratinocytes were differentiated for 7 d in the presence or absence of 10 μM fumonisin B_1. Lipids were extracted, treated with an alkali, and derivatized to AMPP amides. Derivatized FAs were analyzed by a Xevo TQ-S LC/MS system and quantified by MassLynx software. Statistically significant differences are indicated; $*P < 0.05$, $**P < 0.01$; *t* test. hC26:0, hydroxy C26:0 FA. (*B*) Total membrane fractions (50 μg) prepared from BY4741 bearing the pAK1017 (vector) or pNS29 (*His_6-Myc-3xFLAG-CYP4F22*) plasmids were incubated with 10 μM C30:0 FA and 1 mM NADPH as indicated for 1 h at 37 °C. Lipids were extracted, derivatized to AMPP amides, and analyzed as in *A*. The values represent the amount of each FA ω-hydroxylase activity relative to that of the vector/–NADPH sample. The value of the CYP4F22/+NADPH sample was statistically different from the values of all other samples ($**P < 0.01$; *t* test). hC30:0, hydroxy C30:0 FA. (*C* and *D*) HEK 293T cells were transfected with the plasmids encoding *ELOVL1* or *ELOVL4*, *CERS2* or *CERS3*, and *CYP4F22*. Transfected cells were labeled with [^{3}H]sphingosine for 4 h at 37 °C. Extracted lipids were separated by reverse-phase TLC (*C*) or by normal-phase TLC (*D*) and detected by autoradiography. Cer, ceramide; GlcCer, glucosylceramide; SM, sphingomyelin; SPH, sphingosine; ω-OH, ω-hydroxy.

12(*R*)-trioxilin A_3. However, the exact roles of hepoxilins and trioxilins in epidermal barrier formation and/or keratinocyte differentiation are still unclear. Furthermore, recent findings have demonstrated that ALOX12B and ALOXE3 are involved in the reactions necessary for conversion of acylceramide to protein-bound ceramide, i.e., peroxidation of the linoleate moiety and subsequent epoxyalcohol derivatization (13). In addition, ALOX12B was proven not to be involved in hepoxilin/trioxilin production (30). These findings suggest that, although hepoxilin/trioxilin metabolism may not be relevant to the pathogenesis of ichthyosis, the impairment of acylceramide/protein-bound ceramide formation causes ichthyosis. Based on these recent findings, some researchers have predicted that CYP4F22 is involved in acylceramide generation (3, 31), but until now their suppositions have lacked experimental evidence.

We determined the membrane topology of CYP4F22 (Fig. 4*C*), which indicates that the large C-terminal hydrophilic domain including catalytic residues is located in the cytosol. Therefore, ω-hydroxylation of the ULCFA portion of acylceramide must occur on the cytosolic side of the ER membrane. Based on this finding, we propose a working model for the process of acylceramide production in the ER membrane as follows (Fig. S6). Elongation of palmitoyl-CoA to ULCFA-CoA occurs on the cytoplasmic side of the ER membrane. Because lipids comprising the ER membrane are mostly C16 and C18, ULCFA (C28–C36) portions of ULCFA-CoAs should be bent in the cytosolic leaflet of the ER membrane (Fig. S6) or should penetrate into the luminal leaflet. Although the latter possibility cannot be excluded, we prefer the former, because in the latter model ULCFA must flip-flop at least three times in the ER membrane in the course of acylceramide production. Because the substrates of CYP4F22 are ULCFAs (Fig. 5), ULCFA-CoAs should be converted to ULCFAs before ω-hydroxylation. After ω-hydroxylation of ULCFAs by CYP4F22, the resulting ω-hydroxy-ULCFA is converted to ω-hydroxy-ULCFA-CoA by acyl-CoA synthetase. ACSVL4/FATP4 is the candidate acyl-CoA synthetase for this reaction, because *Acsvl4*-mutant mice exhibited skin barrier defects (32). CERS3 catalyzes the formation of ω-hydroxyceramide from ω-hydroxy-ULCFA-CoA and LCB. An unknown acyltransferase then introduces linoleic acid into the ω-hydroxy group of ω-hydroxyceramide, generating acylceramide.

Our results presented here demonstrate, for the first time to our knowledge, that CYP4F22 is a bona fide ULCFA ω-hydroxylase required for acylceramide production. Our findings provide important insights into the molecular mechanisms of skin permeability barrier formation. Future development of compounds that strengthen the skin permeability barrier by increasing acylceramide-synthetic proteins such as ELOVL4, CERS3, and CYP4F22 may be useful for treatment of cutaneous disorders including ichthyosis and atopic dermatitis.

Materials and Methods

Details of the materials and methods used for all procedures are given in *SI Materials and Methods*.

Ethics. Stratum corneum was obtained from an ARCI patient (a 2-y-old girl) (25), carriers (her parents) (mother, 35 y old, c.1138delG; father, 39 y old, c.728G→A), and a healthy control (an 11-y-old girl). This study was approved by the ethical committees of Nagoya University Graduate School of Medicine and the Kao Corporation. Informed consent was obtained from all participants after the procedures had been explained. Informed consents for the girls were obtained from their parents.

Plasmids. Human *CYP4F* subfamily genes and the human *CERS3* gene were amplified by PCR using their respective forward and reverse primers listed in Table S2. The amplified DNAs first were cloned into pGEM-T Easy Vector (Promega) and then were transferred to the pCE-puro 3xFLAG-1 plasmid, a mammalian expression vector designed to produce an N-terminal 3xFLAG-tagged protein.

[^{3}H]Sphingosine Labeling Assay. Cells were labeled with 2 μCi [3-^{3}H]sphingosine (20 Ci/mmol; PerkinElmer Life Sciences) for 4 h at 37 °C. Lipids were extracted as described previously (28, 33) and separated by normal-phase TLC and reverse-phase TLC.

Lipid Analysis Using LC-MS. FAs and ceramides prepared from cultured cells were analyzed by reversed-phase LC/MS using ultra-performance liquid chromatography (UPLC) coupled with electrospray ionization (ESI) tandem triple quadrupole MS (Xevo TQ-S; Waters). Each ceramide species was detected by multiple reaction monitoring (MRM) by selecting the *m/z* ($[M-H_2O+H]^+$ and $[M+H]^+$) of specific ceramide species at Q1 and the *m/z* 264.2 at Q3 (Table S3). FAs were analyzed after derivatization to *N*-(4-aminomethylphenyl)pyridinium (AMPP) amides using the AMP^+ Mass Spectrometry Kit (Cayman Chemical). Hydroxy FA species were detected by MRM by selecting the *m/z* ($[M+H]^+$) of the derivatized hydroxy FA species at Q1 and the *m/z* 238.9 at Q3, corresponding to the fragment cleaved between C3 and C4 of derivatized FAs (Table S3). Stratum corneum ceramides were analyzed by reversed-phase LC/MS using the Agilent 1100 Series LC/MSD SL system (Agilent Technologies). Each ceramide species was detected by selected ion monitoring as *m/z* $[M+CH_3COO]^-$ (Table S4).

Immunoblotting. Immunoblotting was performed as described previously (34, 35) using anti-FLAG M2 (1.85 μg/mL) (Sigma), anti-calnexin 4F10 (1 μg/mL) (Medical & Biological Laboratories), or anti-GAPDH 6C5 (1 μg/mL; Ambion, Life Technologies) antibody as a primary antibody and an HRP-conjugated anti-mouse IgG $F(ab')_2$ fragment (1:7,500 dilution; GE Healthcare Life Sciences) as a secondary antibody. Labeling was detected using Pierce ECL Western Blotting Substrate (Thermo Fisher Scientific).

ACKNOWLEDGMENTS. This work was supported by the Creation of Innovation Centers for Advanced Interdisciplinary Research Areas Program from the Ministry of Education, Culture, Sports, Science and Technology of Japan (A.K.); and Grant-in-Aid for Scientific Research (A) 26251010 (to A.K.) and Grant-in-Aid for Young Scientists (A) 15H05589 (to Y.O.), both from the Japan Society for the Promotion of Science.

1. Uchida Y, Holleran WM (2008) Omega-O-acylceramide, a lipid essential for mammalian survival. *J Dermatol Sci* 51(2):77–87.
2. Mizutani Y, Mitsutake S, Tsuji K, Kihara A, Igarashi Y (2009) Ceramide biosynthesis in keratinocyte and its role in skin function. *Biochimie* 91(6):784–790.
3. Breiden B, Sandhoff K (2014) The role of sphingolipid metabolism in cutaneous permeability barrier formation. *Biochim Biophys Acta* 1841(3):441–452.
4. Kihara A (2012) Very long-chain fatty acids: Elongation, physiology and related disorders. *J Biochem* 152(5):387–395.
5. Sassa T, Kihara A (2014) Metabolism of very long-chain Fatty acids: Genes and pathophysiology. *Biomol Ther (Seoul)* 22(2):83–92.
6. Farwanah H, Wohlrab J, Neubert RH, Raith K (2005) Profiling of human stratum corneum ceramides by means of normal phase LC/APCI-MS. *Anal Bioanal Chem* 383(4): 632–637.
7. Masukawa Y, et al. (2008) Characterization of overall ceramide species in human *stratum corneum*. *J Lipid Res* 49(7):1466–1476.
8. Wertz PW, Cho ES, Downing DT (1983) Effect of essential fatty acid deficiency on the epidermal sphingolipids of the rat. *Biochim Biophys Acta* 753(3):350–355.
9. Imokawa G, et al. (1991) Decreased level of ceramides in stratum corneum of atopic dermatitis: An etiologic factor in atopic dry skin? *J Invest Dermatol* 96(4):523–526.
10. Ishikawa J, et al. (2010) Changes in the ceramide profile of atopic dermatitis patients. *J Invest Dermatol* 130(10):2511–2514.
11. Janssens M, et al. (2012) Increase in short-chain ceramides correlates with an altered lipid organization and decreased barrier function in atopic eczema patients. *J Lipid Res* 53(12):2755–2766.
12. Wertz PW, Downing DT (1987) Covalently bound ω-hydroxyacylsphingosine in the stratum corneum. *Biochim Biophys Acta* 917(1):108–111.
13. Zheng Y, et al. (2011) Lipoxygenases mediate the effect of essential fatty acid in skin barrier formation: A proposed role in releasing omega-hydroxyceramide for construction of the corneocyte lipid envelope. *J Biol Chem* 286(27):24046–24056.
14. Jobard F, et al. (2002) Lipoxygenase-3 (*ALOXE3*) and 12(*R*)-lipoxygenase (*ALOX12B*) are mutated in non-bullous congenital ichthyosiform erythroderma (NCIE) linked to chromosome 17p13.1. *Hum Mol Genet* 11(1):107–113.
15. Eckl KM, et al. (2013) Impaired epidermal ceramide synthesis causes autosomal recessive congenital ichthyosis and reveals the importance of ceramide acyl chain length. *J Invest Dermatol* 133(9):2202–2211.
16. Traupe H, Fischer J, Oji V (2014) Nonsyndromic types of ichthyoses - an update. *J Dtsch Dermatol Ges* 12(2):109–121.
17. Jennemann R, et al. (2012) Loss of ceramide synthase 3 causes lethal skin barrier disruption. *Hum Mol Genet* 21(3):586–608.
18. Krieg P, Fürstenberger G (2014) The role of lipoxygenases in epidermis. *Biochim Biophys Acta* 1841(3):390–400.
19. Akiyama M, Shimizu H (2008) An update on molecular aspects of the non-syndromic ichthyoses. *Exp Dermatol* 17(5):373–382.
20. Aldahmesh MA, et al. (2011) Recessive mutations in *ELOVL4* cause ichthyosis, intellectual disability, and spastic quadriplegia. *Am J Hum Genet* 89(6):745–750.
21. Lefèvre C, et al. (2006) Mutations in a new cytochrome P450 gene in lamellar ichthyosis type 3. *Hum Mol Genet* 15(5):767–776.
22. Behne M, et al. (2000) Omega-hydroxyceramides are required for corneocyte lipid envelope (CLE) formation and normal epidermal permeability barrier function. *J Invest Dermatol* 114(1):185–192.
23. Dhar M, Sepkovic DW, Hirani V, Magnusson RP, Lasker JM (2008) Omega oxidation of 3-hydroxy fatty acids by the human CYP4F gene subfamily enzyme CYP4F11. *J Lipid Res* 49(3):612–624.
24. Sanders RJ, Ofman R, Dacremont G, Wanders RJ, Kemp S (2008) Characterization of the human ω-oxidation pathway for ω-hydroxy-very-long-chain fatty acids. *FASEB J* 22(6):2064–2071.
25. Sugiura K, et al. (2013) Lamellar ichthyosis in a collodion baby caused by *CYP4F22* mutations in a non-consanguineous family outside the Mediterranean. *J Dermatol Sci* 72(2):193–195.
26. Szczesna-Skorupa E, Kemper B (1993) An N-terminal glycosylation signal on cytochrome P450 is restricted to the endoplasmic reticulum in a luminal orientation. *J Biol Chem* 268(3):1757–1762.
27. Shimozawa O, et al. (1993) Core glycosylation of cytochrome P-450(arom). Evidence for localization of N terminus of microsomal cytochrome P-450 in the lumen. *J Biol Chem* 268(28):21399–21402.
28. Ohno Y, et al. (2010) ELOVL1 production of C24 acyl-CoAs is linked to C24 sphingolipid synthesis. *Proc Natl Acad Sci USA* 107(43):18439–18444.
29. Sassa T, et al. (2013) Impaired epidermal permeability barrier in mice lacking *elovl1*, the gene responsible for very-long-chain fatty acid production. *Mol Cell Biol* 33(14): 2787–2796.
30. Krieg P, et al. (2013) *Aloxe3* knockout mice reveal a function of epidermal lipoxygenase-3 as hepoxilin synthase and its pivotal role in barrier formation. *J Invest Dermatol* 133(1):172–180.
31. Elias PM, et al. (2014) Formation and functions of the corneocyte lipid envelope (CLE). *Biochim Biophys Acta* 1841(3):314–318.
32. Moulson CL, et al. (2003) Cloning of wrinkle-free, a previously uncharacterized mouse mutation, reveals crucial roles for fatty acid transport protein 4 in skin and hair development. *Proc Natl Acad Sci USA* 100(9):5274–5279.
33. Nakahara K, et al. (2012) The Sjögren-Larsson syndrome gene encodes a hexadecenal dehydrogenase of the sphingosine 1-phosphate degradation pathway. *Mol Cell* 46(4): 461–471.
34. Kihara A, et al. (2003) Sphingosine-1-phosphate lyase is involved in the differentiation of F9 embryonal carcinoma cells to primitive endoderm. *J Biol Chem* 278(16): 14578–14585.
35. Kitamura T, Takagi S, Naganuma T, Kihara A (2015) Mouse aldehyde dehydrogenase ALDH3B2 is localized to lipid droplets via two C-terminal tryptophan residues and lipid modification. *Biochem J* 465(1):79–87.
36. Brachmann CB, et al. (1998) Designer deletion strains derived from *Saccharomyces cerevisiae* S288C: A useful set of strains and plasmids for PCR-mediated gene disruption and other applications. *Yeast* 14(2):115–132.
37. Kihara A, Sakuraba H, Ikeda M, Denpoh A, Igarashi Y (2008) Membrane topology and essential amino acid residues of Phs1, a 3-hydroxyacyl-CoA dehydratase involved in very long-chain fatty acid elongation. *J Biol Chem* 283(17):11199–11209.
38. Vasireddy V, et al. (2007) Loss of functional ELOVL4 depletes very long-chain fatty acids (≥C28) and the unique ω-O-acylceramides in skin leading to neonatal death. *Hum Mol Genet* 16(5):471–482.
39. Ogawa C, Kihara A, Gokoh M, Igarashi Y (2003) Identification and characterization of a novel human sphingosine-1-phosphate phosphohydrolase, hSPP2. *J Biol Chem* 278(2):1268–1272.
40. Kondo N, et al. (2014) Identification of the phytosphingosine metabolic pathway leading to odd-numbered fatty acids. *Nat Commun* 5:5338.

Disappearance of circulating autoantibodies to RNA polymerase III in a patient with systemic sclerosis successfully treated with corticosteroid and methotrexate

Editor

Although the titres of anti-RNAP III often change in association with total thickness skin score (TSS), it is extremely rare for anti-RNAP III to become negative after treatment in patients with SSc.[1,2]

A 66-year-old man exhibited Raynaud's phenomenon in the fingers. Four months later, oedema of the bilateral hands and feet and polyarthralgia occurred. A half-year after the initial episode of Raynaud's phenomenon, the patient was admitted to our hospital with severe joint pain and the inability to walk unaided. He had no particular past history.

Echocardiography, chest computer tomography, upper gastrointestinal endoscopy and colonoscopy revealed no remarkable finding for heart, lungs and abdomen. His fingers, hands and forearms were swollen with redness, and sclerodermatous skin change was present in the fingers (Fig. 1a). Pitting oedema was observed in the feet (Fig. 1b). The modified Rodnan TSS was 16. The laboratory data were as follows: ESR of 37 mm/h, WBC count of 3740/μL, platelets of 37 300/mm, total protein of 7.1 g/dL, albumin of 2.9 g/dL, blood urea nitrogen of 10 mg/dL, creatinine of 0.59 mg/dL and UA of 3.6 mg/dL, CRP of 5.07 mg/dL, MMP-3 of 39.2 ng/mL (normal range: 36.9–121.0 ng/mL) and plasma renin activity of 3.1 ng/mL/h (normal range: 0.2–3.9 ng/mL/h). Antinuclear antibody (ANA) was positive (1:80; nuclear speckled staining), and anti-RNAP III was detected by enzyme-linked immunosorbent assay (ELISA) with a high index of 104 and 77 at two points (normal range: < 28).[3] Rheumatoid factor, anticyclic citrullinated peptide, anti-SSA/Ro, anti-U1-RNP, anti-Scl-70 and anticentromere antibodies were negative.

A skin biopsy sample obtained from the extensor surface of the forearm showed oedema of the upper and mid dermis (data not shown). Neither bone erosion/destruction nor calcification was seen in the bilateral wrists (Fig. 1c), and there was bone marrow oedema in the carpal bones (Fig. 1d). In light of the above-mentioned findings, the patient was diagnosed as having SSc with anti-RNAP III associated with synovitis.

We administrated systemic prednisolone (PSL) at 30 mg/day, while carefully watching for signs of scleroderma kidney. This achieved almost complete remission of all symptoms, except discomfort of the metacarpophalangeal joints. After tapering the PSL dose by 2.5 mg every 2–3 weeks, the TSS fell to 0 and CRP and ESR levels normalized. When the PSL tapering reached 20 mg/day, the oedema and arthralgia relapsed and the CRP rebounded. After 3 months of PSL treatment, methotrexate (MTX) at 6 mg/week and later at 8 mg/week was added, and the joint symptoms were relieved and the CRP level decreased again. PSL has been tapered to 9 mg, and MTX at 8 mg/week has been continued; however, no recurrence of skin sclerosis or arthralgia, or even of Raynaud's phenomenon has occurred for 2 years. Surprisingly, anti-RNAP III became negative (index value: 10) with ELISA about 1 year after PSL was started (Fig. 2). ANA also became negative.

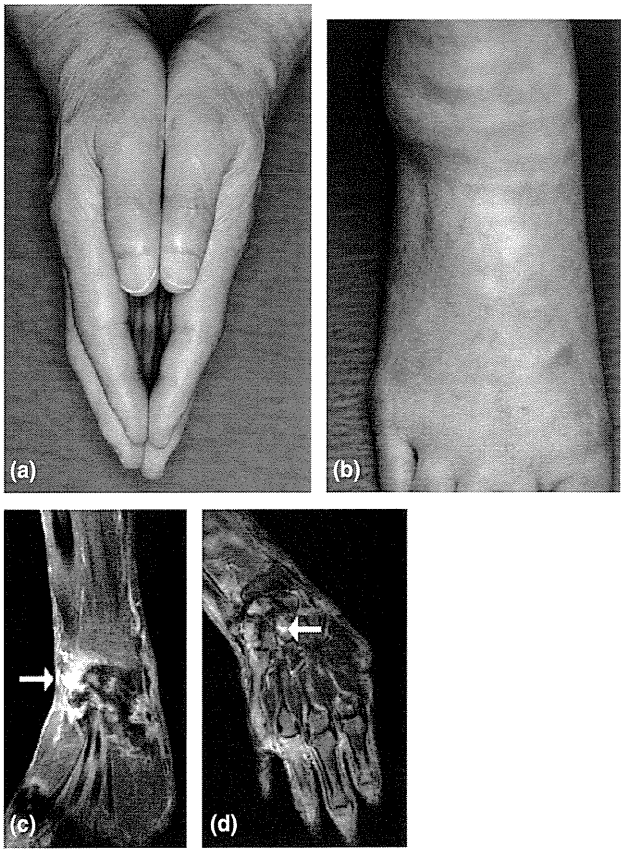

Figure 1 Clinical features of the patient before treatment. (a) The fingers and hands are red and swollen. (b) Pitting oedema is observed in the foot. (c, d) Enhanced MRI on the right hand shows synovitis (c: fat-suppressed images with gadolinium contrast agent) and bone oedema (d: high signal intensity on short tau inversion recovery).

We do not know the exact mechanism of how the antibodies disappeared in this case, although we assume that the extremely positive response to the treatments for SSc, to the extent of completely resolving the Raynaud's phenomenon, might be related to the disappearance of anti-RNAP III. The disappearance of anti-MDA-5 autoantibodies in clinically amyopathic dermatomyositis/interstitial lung disease during disease remission is

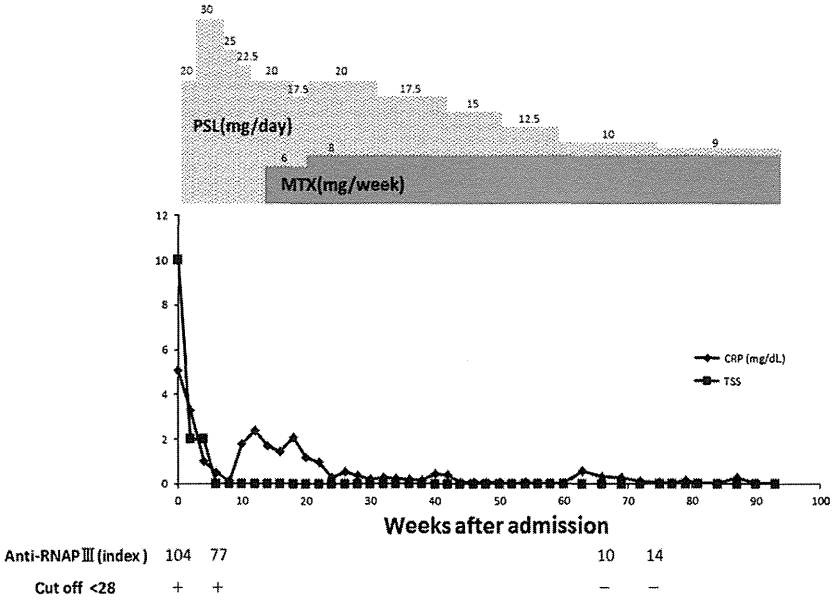

Figure 2 The treatment, course and circulating anti-RNAP III antibody titres of the patient.

another example of the disappearance of autoantibodies in a rheumatic disease.[4]

In conclusion, this is the first clear demonstration that anti-RNAP III can become negative after successful treatments in SSc patients with circulating anti-RNAP III antibodies. The present case gives us useful information that disappearance of anti-RNAP III autoantibodies might be a marker for disease remission in SSc patients with anti-RNAP III antibodies.

Acknowledgements

This study was supported in part by Grant-in-Aid for Scientific Research (C) 23591617 (to K. S.) and Grant-in-Aid for Scientific Research (A) 23249058 (to M.A.), both from the Ministry of Education, Culture, Sports, Science and Technology of Japan.

K. Tanahashi, K. Sugiura,* Y. Muro, M. Akiyama
Department of Dermatology, Nagoya University Graduate School of Medicine, Nagoya, Japan

*Correspondence: K. Sugiura. E-mail: kazusugi@med.nagoya-u.ac.jp

References

1 Kuwana M, Okano Y, Pandey JP *et al.* Enzyme-linked immunosorbent assay for detection of anti-RNA polymerase III antibody: analytical accuracy and clinical associations in systemic sclerosis. *Arth Rheum* 2005; **52**: 2425–2432.
2 Nihtyanova SI, Parker JC, Black CM, Bunn CC, Denton CP. A longitudinal study of anti-RNA polymerase III antibody levels in systemic sclerosis. *Rheumatology (Oxford)* 2009; **48**: 1218–1221.
3 Satoh T, Ishikawa O, Ihn H *et al.* Clinical usefulness of anti-RNA polymerase III antibody measurement by enzyme-linked immunosorbent assay. *Rheumatology (Oxford)* 2009; **48**: 1570–1574.
4 Muro Y, Sugiura K, Hoshino K, Akiyama M. Disappearance of anti-MDA-5 autoantibodies in clinically amyopathic DM/interstitial lung disease during disease remission. *Rheumatology (Oxford)* 2012; **51**: 800–804.

DOI: 10.1111/jdv.12512

[1]Ueo Dermatology Clinic, Saiki, Oita 876-0831, Japan
[2]Department of Dermatology, Kurume University School of Medicine, and Kurume University Institute of Cutaneous Cell Biology, Kurume, Fukuoka 830-0011, Japan
[3]Department of Dermatology, Faculty of Medicine, Oita University, Hasama, Yufu, Oita 879-5593, Japan
Correspondence: Sakuhei Fujiwara.
E-mail: fujiwara@oita-u.ac.jp

D. Ueo[1]
N. Ishii[2]
T. Hamada[2]
K. Teye[2]
T. Hashimoto[2]
Y. Hatano[3]
S. Fujiwara[3]

References

1 Hamada T, Fukuda S, Sakaguchi S *et al.* Molecular and clinical characterization in Japanese and Korean patients with Hailey–Hailey disease: six new mutations in the ATP2C1 gene. *J Dermatol Sci* 2008; **51**:31–6.
2 Makhneva N, Beletskaya LV. Fixed and soluble immune complexes in the epidermis in Hailey–Hailey disease. *J Dermatol* 2007; **34**:410–12.
3 Bennani I, Ofaiche J, Uthurriague C *et al.* [Antidesmoglein antibodies in a patient with Hailey–Hailey disease]. *Ann Dermatol Venereol* 2012; **139**:621–5 (in French).
4 Tateishi C, Tsuruta D, Nakanishi T *et al.* Antidesmocollin-1 antibody-positive, antidesmoglein antibody-negative pemphigus herpetiformis. *J Am Acad Dermatol* 2010; **63**:e8–10.
5 Endo Y, Tsujioka K, Tanioka M *et al.* Bullous dermatosis associated with IgG antibodies specific for desmocollins. *Eur J Dermatol* 2010; **20**:620–5.
6 Zhang D, Li X, Xiao S *et al.* Detection and comparison of two types of ATP2C1 gene mutations in Chinese patients with Hailey–Hailey disease. *Arch Dermatol Res* 2012; **304**:163–70.
7 Cialfi S, Oliviero C, Ceccarelli S *et al.* Complex multipathways alterations and oxidative stress are associated with Hailey–Hailey disease. *Br J Dermatol* 2010; **162**:518–26.

Funding sources: none.

Conflicts of interest: none declared.

The novel *GJB3* mutation p.Thr202Asn in the M4 transmembrane domain underlies erythrokeratodermia variabilis

DOI: 10.1111/bjd.13641

Dear Editor, Erythrokeratodermia variabilis (EKV; OMIM 133200) is a rare autosomal dominant disorder characterized by migratory erythematous areas and fixed keratotic plaques. *GJB3* and *GJB4*, which encode connexin (Cx)31 and Cx30.3, respectively, are causative genes for EKV and nonsyndromic hearing loss.[1,2] Here, we report a single novel mutation of *GJB3*, p.Thr202Asn, in the M4 transmembrane domain in a Japanese family suffering from EKV. In addition, we review the literature and characterize the possible genotype–phenotype correlations for *GJB3* mutations. Specifically, missense mutations, other than those in the second extracellular loop (E2) domain, are associated with EKV and those in the E2 domain underlie autosomal dominant nonsyndromic hearing loss (ADNSHL).

A 17-year-old girl presented with palmoplantar keratoderma (PPK), which had been noted since infancy. Physical examination showed variably sized and irregularly shaped erythema, with scaling on the trunk and the extremities (Fig. 1a). These lesions were transient, but reappeared repeatedly. Notable PPK was also observed (Fig. 1b). She had no hearing loss and refused to undergo hearing tests. Histological examination showed hyperkeratosis with intact granular layers. Her paternal grandfather, father and sister showed similar clinical features (Fig. 1c). Clinical and histological features supported the diagnosis of EKV.

After ethical approval was granted, written informed consent was obtained from the participants, in compliance with the Declaration of Helsinki. The coding regions, including the exon–intron boundaries of *GJB3* and *GJB4*, were amplified by polymerase chain reaction from genomic DNA obtained from the participants, as described previously.[1,2] The mutation analysis revealed that the proband, her father and her sister harboured the heterozygous mutation p.Thr202Asn

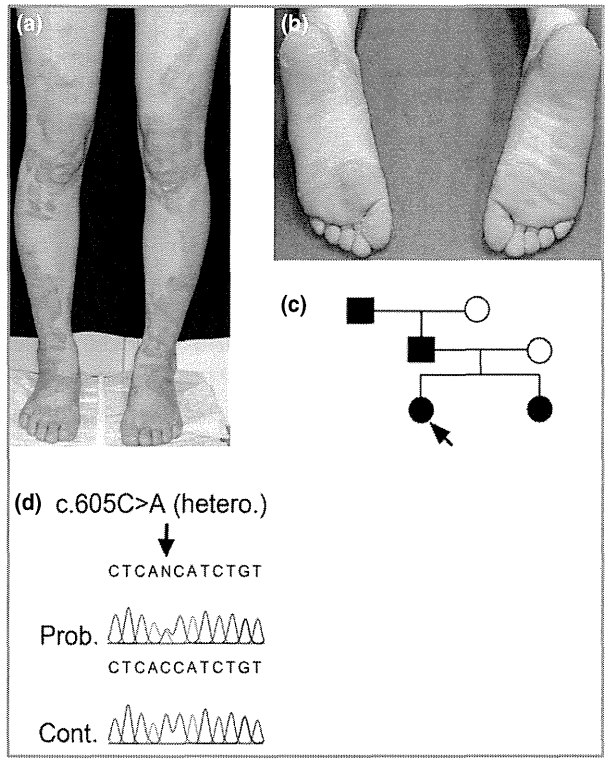

Fig 1. Clinical features of the proband (Prob.), family pedigree and sequence data for GJB3. (a) Persistent indurated erythematous plaques on the lower limbs. (b) Hyperkeratotic skin on the soles. (c) Pedigree of the proband's family. (d) Sequence of *GJB3* for the proband and control (Cont.).

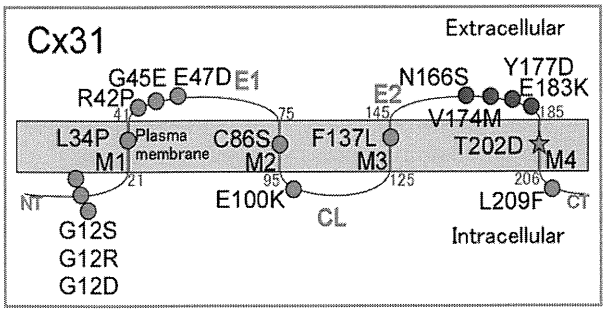

Fig 2. Reported causative dominant pathogenic missense mutations for erythrokeratodermia variabilis (EKV) and autosomal dominant nonsyndromic hearing loss (ADNSHL) in connexin (Cx)31. Only dominant missense mutations in the E2 domain underlie ADNSHL (blue circles), and all dominant pathogenic missense mutations outside the E2 domain cause EKV (red circles and asterisk). Residues at the boundaries between the functional domains are indicated by green numbers. M1–M4, transmembrane domains 1–4; E1, extracellular domain 1; E2, extracellular domains 2; CL, cytoplasmic loop; NT, N terminus; CT, C terminus.

(c.605C>A) in *GJB3*, while her mother did not (Fig. 1d). MutationTaster (http://www.mutationtaster.org/) predicted that p.Thr202Asn was a disease-causing allele. p.Thr202Asn is not reported in the Exome Sequencing Project of the Human Genetic Variation Browser (http://www.genome.med.kyoto-u.ac.jp/SnpDB/), which is a database of genetic variants in > 1400 Japanese individuals. Thus, the proband and her affected family members were diagnosed as having EKV with the heterozygous *GJB3* mutation.

Cxs are highly homologous and comprise a large gene family encoding plasma membrane proteins.[3] Cxs contain four transmembrane domains linked by one cytoplasmic and two extracellular loops; N and C termini are located on the cytoplasmic side (Fig. 2). The transmembrane domains bear conserved amino acids, whereas the cytoplasmic loop and the C-terminal region are highly variable among Cxs. Cxs are assembled in groups of six to form hemichannels in the plasma membrane, and two hemichannels of adjacent cells then combine to form a gap junction. Various Cxs combine into homomeric and heteromeric gap junctions.

Cx31 is expressed in the upper differentiating epidermal layers.[4] In addition to the epidermis, it is expressed in the cochlea, and some mutations are involved in hearing loss without obvious cutaneous phenotypes.[5] Figure 2 summarizes the *GJB3* missense mutant alleles reported thus far, including that of the present case, and their associations with EKV or ADNSHL, according to the Human Gene Mutation Database of the Institute of Medical Genetics, Cardiff, U.K. (http://www.hgmd.cf.ac.uk/ac/index.php). p.Thr202Asn is the first autosomal dominant missense mutation reported in the M4 domain; it was the only remaining domain of Cx31 for which no pathogenic autosomal dominant mutations were reported (Fig. 2). Interestingly, all missense mutations in any domain other than E2 were associated with EKV. In contrast, all missense mutations in the E2 domain were associated with ADNSHL. Figure S1 (see Supporting Information) shows the sequence alignment of the E2 domain for diverse vertebrate species. p.174Val, p.177Tyr and p.183Glu are conserved among vertebrate species, but p.166Asn is not. Based on a review of *GJB3*-associated autosomal recessive nonsyndromic hearing loss, *GJB3* missense mutations have been reported that are not located in the E2 domain (http://www.hgmd.cf.ac.uk/ac/index.php).

We assume different pathogenic mechanisms determine the phenotypes associated with *GJB3* dominant missense mutations in the E2 domain and those outside the E2 domain. The E1 domain is important for the formation of the gap junction channel, and the E2 domain is important for docking compatibility in heterotypic channels in many members of the Cx family.[3] Indeed, one of the missense mutations in the E2 domain of Cx31 reportedly has no effect on the function of wild-type Cx31 but interferes with Cx26 function.[6] Of all the Cxs, malfunction of Cx26 most frequently results in hearing loss.[7] In this context, we suspect that dominant missense mutations in the E2 domain of *GJB3* might cause hearing loss via dysfunction of Cx26.

In summary, to our knowledge, we have identified the first dominant pathogenic missense mutation in the M4 transmembrane domain of *GJB3*. As was the case for other *GJB3* dominant pathogenic missense mutations outside the E2 domain, the mutation led to the EKV phenotype in the patient's family. Our results, combined with a literature review, suggest that dominant missense mutations outside the E2 domain in *GJB3* are associated with EKV, and those within the E2 domain cause ADNSHL.

Acknowledgments

We thank Ms Haruka Ozeki and Ms Yuka Terashita for their technical help in analysing the *GJB3* and *GJB4* mutations.

[1]*Department of Dermatology, Nagoya University Graduate School of Medicine, 65 Tsurumai-cho, Showa-ku, Nagoya, Aichi 466-8550, Japan*
[2]*Department of Dermatology, Fujita Health University School of Medicine, 1-98 Dengakugakubo, Kutsukake-cho, Toyoake, Aichi 470-1192, Japan*
Correspondence: Masashi Akiyama.
E-mail: makiyama@med.nagoya-u.ac.jp

K. Sugiura[1]
M. Arima[2]
K. Matsunaga[2]
M. Akiyama[1]

References

1 Richard G, Smith LE, Bailey RA *et al.* Mutations in the human connexin gene *GJB3* cause erythrokeratodermia variabilis. *Nat Genet* 1998; **20**:366–9.
2 Macari F, Landau M, Cousin P *et al.* Mutation in the gene for connexin 30.3 in a family with erythrokeratodermia variabilis. *Am J Hum Genet* 2000; **67**:1296–301.

3 Bai D, Wang AH. Extracellular domains play different roles in gap junction formation and docking compatibility. *Biochem J* 2014; **458**:1–10.
4 Di WL, Rugg EL, Leigh IM *et al.* Multiple epidermal connexins are expressed in different keratinocyte subpopulations including connexin 31. *J Invest Dermatol* 2001; **117**:958–64.
5 Kelsell DP, Di WL, Houseman MJ. Connexin mutations in skin disease and hearing loss. *Am J Hum Genet* 2001; **68**:559–68.
6 Li TC, Kuan YH, Ko TY *et al.* Mechanism of a novel missense mutation, p. V174M, of the human connexin31 (GJB3) in causing nonsyndromic hearing loss. *Biochem Cell Biol* 2014; **92**:251–7.
7 Xu J, Nicholson BJ. The role of connexins in ear and skin physiology – functional insights from disease-associated mutations. *Biochim Biophys Acta* 2013; **1828**:167–78.

Funding sources: This study was supported, in part, by a Grant-in-Aid for Challenging Exploratory Research 26670526 (to K.S.) and a Grant-in-Aid for Scientific Research (A) 23249058 (to M.Ak), both from the Ministry of Education, Culture, Sports, Science, and Technology of Japan.

Conflicts of interest: none declared.

Supporting Information

Additional Supporting Information may be found in the online version of this article at the publisher's website:

Fig S1. Sequence alignment of the E2 domain of Cx31 in diverse vertebrate species.

Dermatitis induced by first-generation hepatitis C virus protease inhibitors

DOI: 10.1111/bjd.13694

Dear Editor, We read with great interest the U.K. experience of the cutaneous side-effects of first-generation hepatitis C virus (HCV) protease inhibitors.[1] The majority of the side-effects are mild-to-moderate and are generally similar to those observed with peginterferon-α (PEG-IFN)/ribavirin, including xerosis, pruritus and eczema.[1,2] The authors stated that these adverse reactions had a class effect but they did not discuss the pathophysiology.

It is remarkable that these dermatological manifestations were already known in patients with untreated chronic hepatitis C. However, their frequency increased with the use of IFN and became more frequent with the development of a PEG-IFN/ribavirin schedule. We previously studied the prevalence of skin manifestations in patients with chronic hepatitis C at the Department of Hepatology, Beaujon Hospital, Clichy, France, in 2003.[3] Xerosis, pruritus and eczema were observed in 14%, 6% and 7% of the patients not receiving any treatment (n = 98) and in 49%, 48% and 19% in patients treated with PEG-IFN/ribavirin (n = 108 patients), respectively. Recent data have demonstrated that the use of telaprevir and boceprevir dramatically increased their frequency.

Antiproteases may have a direct effect on keratinocytes and stratum corneum but we propose that these antiproteases may favour immune reconstitution. These adverse reactions may be related to the IFN pathway. Telaprevir and boceprevir are targeted to the NS3/NS4 proteases. These nonstructural proteins are not only necessary for virus replication, but are also responsible for the 'immune evasion' of HCV.[4] The NS3/NS4 complex has been described to suppress activation of IFN regulatory factor 3 (IRF-3), a central antiviral transcription factor.[5] IRF-3 promotes the production of IFN and regulates many of the IFN-stimulated genes in response to viral infection. We assume that in addition to antiviral specific action, protease inhibitors such as telaprevir may increase IFN efficacy (produced by, and administrated to, the patient), and may also increase the adverse skin reactions associated with IFN. In this regard, new direct acting antiviral agents against HCV do not target NS3/NS4 and have fewer cutaneous side-effects (Table 1).[6–10]

Acknowledgments

We are indebted to Patrick Marcellin (Beaujon Hospital, Clichy, France).

Table 1 Prevalence of adverse skin reactions in some pivotal studies with telaprevir, boceprevir, sofosbuvir and ledipasvir

Previous treatment	Telaprevir (previously treated)[6]		Boceprevir (previously treated)[7]		Ledipasvir–sofosbuvir (untreated)[8]		Ledipasvir–sofosbuvir (previously treated)[9]		Sofosbuvir (untreated)[10]		
Regimen	PEG-IFN/ ribavirin (48 weeks)	PEG-IFN/ ribavirin/ telaprevir (48/24 weeks)	PEG-IFN/ ribavirin (44 weeks)	PEG-IFN/ ribavirin/ boceprevir (44 weeks)[a]	Ribavirin/ ledipasvir/ sofosbivir (24 weeks)[b]	Ledipasvir/ sofosbivir (24 weeks)	Ribavirin/ ledipasvir/ sofosbivir (24 weeks)	Ledipasvir/ sofosbivir (24 weeks)	PEG-IFN/ ribavirin (24 weeks)	PEG-IFN/ ribavirin/ sofosbivir (12 weeks)	Ribavirin/ sofosbivir (12 weeks)
Dry skin (%)	ND	ND	8	22	ND	ND	10	3	ND	ND	ND
Pruritus (%)	15	44	ND	ND	12	7	ND	ND	17	17	7
Rash (%)	20	60	5	14	12	7	14	6	18	18	9

PEG-IFN, peginterferon-α; ND, no data. [a]Ledipasvir is hepatitis C virus NS5A inhibitor; [b]Sofosbivir is a nucleotide analogue of the hepatitis C virus NS5B polymerase inhibitor.

CED
Clinical and Experimental Dermatology

Ichthyosis follicularis, atrichia, and photophobia syndrome associated with a new mutation in *MBTPS2*

K. Fong,[1] T. Takeichi,[1,2] L. Liu,[3] R. Pramanik,[1] J. Lee,[1] M. Akiyama[2] and J. A. McGrath[1]

[1]*St John's Institute of Dermatology, King's College London (Guy's Campus), London, UK;* [2]*Department of Dermatology, Nagoya University Graduate School of Medicine, Nagoya, Japan; and* [3]*Viapath, St Thomas' Hospital, London, UK*

doi:10.1111/ced.12587

Summary

Ichthyosis follicularis, atrichia and photophobia (IFAP) syndrome (OMIM 308205) is a rare X-linked genetic disorder. Mutations in *MBTPS2* underlie IFAP syndrome, with 19 different mutations reported to date. Keratosis follicularis spinulosa decalvans (KFSD) is an allelic disorder that results from a single recurrent mutation, p.Asn508Ser. We report a case from the UK of IFAP syndrome resulting from a new mutation, p.Asn508Thr, emphasizing the significant overlap between IFAP and KFSD at both the molecular and clinical levels. An area of alopecia on the scalp of the proband's mother was also noted, suggesting lyonization.

Ichthyosis follicularis, atrichia and photophobia (IFAP) syndrome (OMIM 308205) is a rare X-linked genetic skin disorder. The disease severity varies, ranging from mild cases limited to the skin, to the severe BRESHECK variant involving multiple extracutaneous features (brain anomalies, retardation, ectodermal dysplasia, skeletal deformities, Hirschsprung disease, ear/eye anomalies, cleft palate/cryptorchidism, and kidney dysplasia/hypoplasia). In 2009, mutations in *MBTPS2* (membrane-bound transcription factor peptidase, site 2; OMIM 300294) located on chromosome Xp22.1 were identified as the genetic basis for IFAP syndrome.[1] To date, approximately 19 different mutations have been described in this gene. Here, we report a case from the UK of IFAP syndrome resulting from a new missense mutation in *MBTPS2*.

Correspondence: Dr John McGrath, Dermatology Research Laboratories, 9th Floor, Tower Wing, Guy's Hospital, Great Maze Pond, London SE1 9RT, UK
E-mail: john.mcgrath@kcl.ac.uk

Conflict of interest: the authors declare that they have no conflicts of interest.

The first two authors contributed equally to this work and should be considered joint first authors.

Accepted for publication 25 August 2014

Report

The proband was a 5-year-old boy, born to non-consanguineous parents, who was referred for assessment of hair loss and roughened skin texture (Fig. 1). His mother recalled that the child had normal-appearing scalp hair at birth but congenital absence of eyebrows or eyelashes. His scalp hair was then lost over a period of a few days when he was 1 month of age. Since then, a few small scalp hairs had grown, but these were short and easily shed. A few eyelashes had also developed over the past year. In addition, he had developed a rough texture to part of his face, particularly around the eyebrows, and exhibited photophobia. There were no problems noted in his sweating, dentition or nail development. Intellectual development was normal, and he was coping well in school. He had a younger brother with none of these symptoms.

Physical examination revealed complete alopecia with spiny rough skin on the child's eyebrows and evident erythrokeratoderma on both cheeks. There was moderate keratosis pilaris on the child's arms and legs, and a few similar papules on his trunk. Clinically, the features were suggestive of IFAP syndrome. Of note, the patient's mother was also noted to have mild keratosis pilaris and a small area of congenital alopecia on her crown (Fig. 3a). No unusual findings were seen from clinical examination of the patient's father and younger sibling.

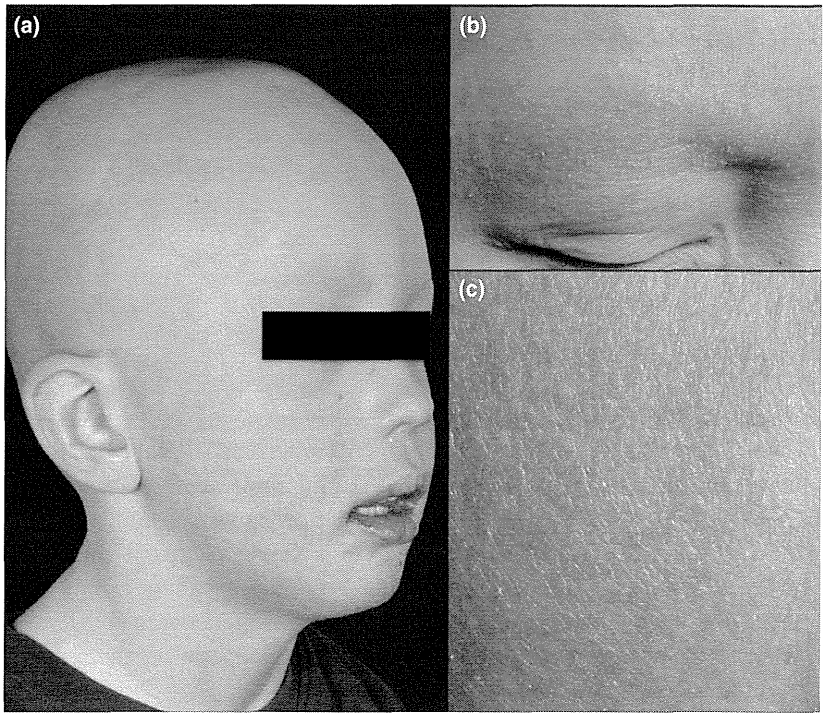

Figure 1 Child with ichthyosis follicularis, atrichia, and photophobia syndrome, showing (a) complete alopecia affecting the scalp and eyebrows and erythrokeratoderma of the cheeks; and (b) roughened skin, particularly affecting the eyebrow region. (c) Closer view of erythrokeratoderma and roughened texture of the cheeks.

The proband and his parents were screened for mutations in *MBTPS2*. The study was approved by the research ethics committee of the Guy's and St Thomas' Hospital NHS Foundation Trust, and conducted according to the principles of the Declaration of Helsinki. Written informed consent was obtained from all participants.

Peripheral blood was sampled from all three individuals for genomic DNA extraction and *MBTPS2* sequencing. PCR amplification of genomic DNA was performed using 12 primer pairs spanning the coding exons and flanking introns of *MBTPS2*, as described previously.[1] The PCR products were purified (QIAquick PCR Purification kit; Qiagen, Crawley, Sussex, UK) and sequenced on an automatic analyser (ABI 3730 Genetic Analyser; Applied Biosystems, Warrington, Cheshire, UK). Bidirectional sequencing identified an A>C transversion mutation at position c.1523, which converts asparagine to threonine (p.Asn508Thr) (Fig. 2). Using *in silico* bioanalysis tools, this missense mutation was predicted to be probably damaging by PolyPhen-2 (score 1) and damaging by SIFT (Sorting Intolerant From Tolerant; score 0), and was not identified in screening of 220 control chromosomes. The proband's father and mother were found to be wild-type and heterozygous for the mutation, respectively, consistent with the X-linked nature of IFAP syndrome.

To ascertain whether the mother's patch of alopecia was a consequence of lyonization, a 3 mm punch biopsy was taken from the site for DNA and RNA extraction. cDNA was synthesized from RNA (SuperScript III Reverse Transcriptase; Invitrogen, Paisley, Renfrewshire, UK) and both DNA and cDNA samples were sequenced for the mutation c.1523A>C. Sequencing of skin-derived DNA revealed a heterozygous change, similar to the DNA from peripheral blood. Sequencing of cDNA, however, revealed a distinct difference in the chromatogram peak heights at that position, suggesting a predominance of the mutant C nucleotide (Fig. 3b).

MBTPS2 encodes site-2 protease (S2P), a membrane-embedded zinc metalloprotease vital for cholesterol homeostasis via the cleavage of sterol regulatory element-binding proteins (SREBPs) into fragments that function as downstream transcription factors.[2] S2P also functions as a putative endoplasmic reticulum stress sensor through regulation of the unfolded protein response. Defects in these pathways are thought to impair cholesterol and other lipid biochemical pathways in the skin, resulting in aberrant epidermal differentiation.

In addition to causing IFAP syndrome, mutations in *MBTPS2* have also been shown to underlie keratosis follicularis spinulosa decalvans (KFSD; OMIM 308800), and an X-linked form of Olmsted-like syndrome.[3,4] A recent review by Bornholdt *et al.*[5] revealed possible correlations between specific *MBTPS2* mutations and disease phenotypes. Notably, *MBTPS2*

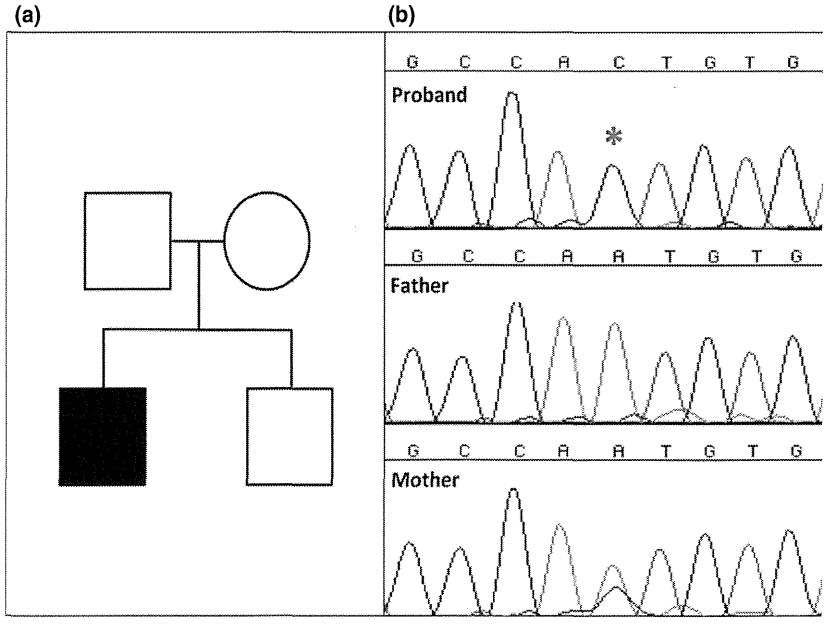

Figure 2 (a) Pedigree showing X-linked nature of ichthyosis follicularis, atrichia, and photophobia syndrome. (b) Genomic sequencing revealed a c.1523A>C transversion in the proband. The father was found to have the wild-type gene, and the mother was heterozygous for the mutation. DNA from the younger brother was not available for testing. *indicates mutant C nucleotide.

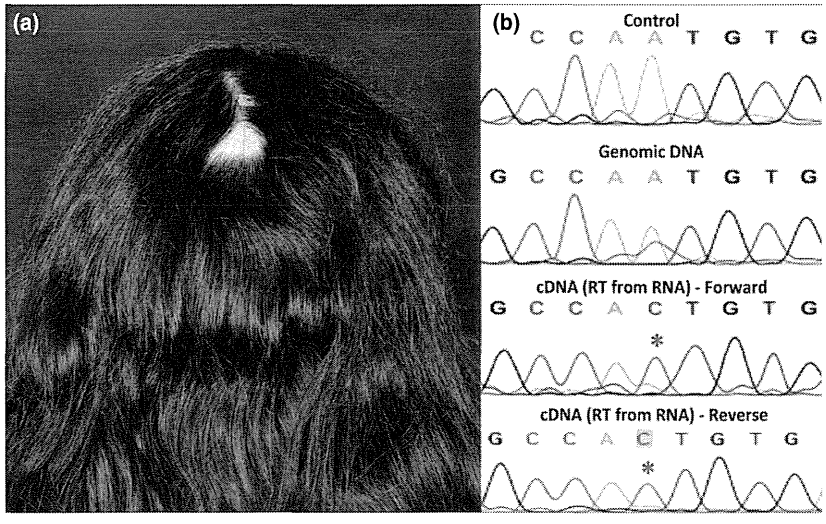

Figure 3 (a) Patch of congenital alopecia affecting the mother's scalp vertex. (b) Sanger sequencing of DNA and cDNA derived from a skin biopsy taken from the site of alopecia revealed the mutation c.1523A>C in a heterozygous state at DNA level (right, second trace), but a predominance of the mutant C allele at the cDNA level (right, bottom two traces). *indicates mutant C nucleotide.

mutations cluster largely within the transmembrane (TM) domains, with mutations in TM7 associated with the BRESHECK variant of IFAP. This severe phenotype is thought to result from the proximity of underlying mutations to the LDG motif, one of two catalytic centres of the S2P enzyme.[6] In contrast to the 20 distinct pathogenic mutations now described in association with IFAP syndrome, the molecular pathology of KFSD and X-linked Olmsted-like syndrome is associated with a single mutation in each: p.Asn508Ser and p.Phe464Ser, respectively. The mutation p.Asn508Thr identified in this study is located in TM8, and results in a relatively mild phenotype of IFAP syndrome limited to the skin/scalp. This same amino acid is also affected by the recurrent mutation p.Asn508Ser, which has been reported in association with both IFAP syndrome and KFSD.[7,8] Although thought to be distinguishable by the presence of cicatricial alopecia, unlike the nonscarring alopecia seen in IFAP syndrome, KFSD shares multiple overlapping clinical features with IFAP syndrome, and a unifying term, IFAP/KFSD syndrome, has been proposed.[3] This study further emphasizes the overlap between both conditions at both a clinical and molecular level.

It has previously been proposed that female carriers of *MBTPS2* mutations may exhibit linear atrophodermic lesions or patches of alopecia, resulting from lyonization, or clonal skewed X-inactivation.[9,10] In this study, Sanger sequencing of DNA and cDNA derived from tissue biopsy at the site of alopecia demonstrated

a predominance of the mutant allele only in the cDNA, suggesting that this change occurs at the RNA rather than DNA level. Although our findings support lyonization as the underlying mechanism, further X-inactivation studies will be required to exclude alternative naevoid pathology unrelated to aberrant *MBTPS2* expression.

In summary, this study has identified a novel *MBTPS2* mutation, c.1523A>C, in a patient from the UK with IFAP syndrome. The case outlines the typical clinical features in an affected male, highlights a possible manifestation of lyonization in his heterozygous mother, extends the spectrum of *MBTPS2* mutations, and further illustrates the clinical and genetic overlap between IFAP syndrome and KFSD.

Learning points

- IFAP syndrome is an X-linked recessive condition resulting from mutations in *MBTPS2*.
- Clinical features of IFAP syndrome include follicular ichthyosis, atrichia and photophobia.
- There is a clinically more severe variant called BRESHECK, associated with multiple extracutaneous abnormalities.
- Mutations in *MBTPS2* can also result in KFSD and X-linked Olmsted-like syndrome.
- IFAP syndrome and KFSD share multiple common features at both the clinical and molecular levels.
- Female carriers of *MBTPS2* mutations can exhibit focal or Blaschko-linear lesions, reflecting lyonization or clonal skewed X-inactivation.

Acknowledgements

This study was supported by the Department of Health via the National Institute for Health Research (NIHR) Comprehensive Biomedical Research Centre award to Guy's & St Thomas' NHS Foundation Trust in partnership with King's College London and King's College Hospital NHS Foundation Trust.

References

1 Oeffner F, Fischer G, Happle R *et al.* IFAP syndrome is caused by deficiency in MBTPS2, an intramembrane zinc metalloprotease essential for cholesterol homeostasis and ER stress response. *Am J Hum Genet* 2009; **84**: 459–67.
2 Sakai J, Duncan EA, Rawson RB *et al.* Sterol-regulated release of SREBP-2 from cell membranes requires two sequential cleavages, one within a transmembrane segment. *Cell* 1996; **85**: 1037–46.
3 Aten E, Brasz LC, Bornholdt D *et al.* Keratosis follicularis spinulosa decalvans is caused by mutations in MBTPS2. *Hum Mutat* 2010; **31**: 1125–33.
4 Haghighi A, Scott CA, Poon DS *et al.* A missense mutation in the MBTPS2 gene underlies the X-linked form of Olmsted syndrome. *J Invest Dermatol* 2013; **133**: 571–3.
5 Bornholdt D, Atkinson TP, Bouadjar B *et al.* Genotype-phenotype correlations emerging from the identification of missense mutations in MBTPS2. *Hum Mutat* 2013; **34**: 587–94.
6 Zelenski NG, Rawson RB, Brown MS, Goldstein JL. Membrane topology of S2P, a protein required for intramembranous cleavage of sterol regulatory element-binding proteins. *J Biol Chem* 1999; **274**: 21973–80.
7 Ding YG, Wang JY, Qiao JJ *et al.* A novel mutation in MBTPS2 causes ichthyosis follicularis, alopecia and photophobia (IFAP) syndrome in a Chinese family. *Br J Dermatol* 2010; **163**: 886–9.
8 Fong K, Wedgeworth EK, Lai-Cheong JE *et al.* MBTPS2 mutation in a British pedigree with keratosis follicularis spinulosa decalvans. *Clin Exp Dermatol* 2012; **37**: 631–4.
9 Konig A, Happle R. Linear lesions reflecting lyonization in women heterozygous for IFAP syndrome (ichthyosis follicularis with atrichia and photophobia). *Am J Med Genet* 1999; **85**: 365–8.
10 Wang HJ, Tang ZL, Lin ZM *et al.* Recurrent splice-site mutation in MBTPS2 underlying IFAP syndrome with Olmsted syndrome-like features in a Chinese patient. *Clin Exp Dermatol* 2014; **39**: 158–61.

Journal of Dermatological Science 79 (2015) 4–9

Contents lists available at ScienceDirect

Journal of Dermatological Science

journal homepage: www.jdsjournal.com

Invited review article

Update on autosomal recessive congenital ichthyosis: mRNA analysis using hair samples is a powerful tool for genetic diagnosis

Kazumitsu Sugiura, Masashi Akiyama *

Department of Dermatology, Nagoya University Graduate School of Medicine, 65 Tsurumai-cho, Showa-ku, Nagoya 466-8550, Japan

ARTICLE INFO

Article history:
Received 10 April 2015
Accepted 20 April 2015

Keywords:
ABCA12 promoter
Autosomal recessive congenital ichthyosis
Congenital ichthyosiform erythroderma
Harlequin ichthyosis
Hair samples
Lamellar ichthyosis

ABSTRACT

Research on the molecular genetics and pathomechanisms of autosomal recessive congenital ichthyosis (ARCI) has advanced considerably and several causative genes and molecules underlying the disease have been identified. Three major ARCI phenotypes are harlequin ichthyosis (HI), lamellar ichthyosis (LI), and congenital ichthyosiform erythroderma (CIE). Skin barrier defects are involved in the pathogenesis of ARCI. In this review, the causative genes of ARCI and its phenotypes as well as recent advances in the field are summarized. The known causative molecules underlying ARCI include *ABCA12*, *TGM1*, *ALOXE3*, *ALOX12B*, *NIPAL4*, *CYP4F22*, *PNPLA1*, *CERS3*, and *LIPN*. It is important to examine genetic associations and to elucidate the pathomechanisms of ARCI to establish effective therapies and beneficial genetic counseling. Next-generation sequencing is a promising method that enables the detection of causative disease mutations, even in cases of unexpected concomitant genetic diseases. For genetic diagnosis, obtaining mRNA from hair follicle epithelial cells, which are analogous to keratinocytes in the interfollicular epidermis, is convenient and minimally invasive in patients with ARCI. We confirmed that our mRNA analysis method using hair follicle samples can be applied not only to keratinization disorders, but also to other genetic diseases in the dermatology field. Studies that suggest potential next-generation therapies using ARCI model mice are also reviewed.

Contents

Abbreviations: ABHD5, α/β hydrolase domain-containing 5; ARCI, autosomal recessive congenital ichthyosis; CBs, collodion babies; CERS3, ceramide synthase 3; CIE, congenital ichthyosiform erythroderma; CGI-58, comparative gene identification 58; CYP4F22, cytochrome P450, family F polypeptide 2 homolog of leukotriene B4-omega-hydroxylase; eLOX-3, lipoxygenase-3; HI, harlequin ichthyosis; FATP4, fatty acid transport protein 4; LG, lamellar granule; LI, lamellar ichthyosis; LIPN, lipase N; NIPAL4, Nipa-like domain-containing 4; PNPLA1, patatin-like phospholipase domain protein 1; SHCB, self-healing collodion baby; TGase, transglutaminase; 12R-LOX, 12(R)-lipoxygenase.

* Corresponding author. Tel.: +81 52 744 2314; fax: +81 52 744 2318.
E-mail address: makiyama@med.nagoya-u.ac.jp (M. Akiyama).

http://dx.doi.org/10.1016/j.jdermsci.2015.04.009
0923-1811/

1. Introduction

Autosomal recessive congenital ichthyosis (ARCI) is a heterogeneous group of keratinization disorders characterized primarily by abnormal skin scaling over the whole body [1]. These disorders are limited to the skin, and more than half of all patients present severe symptoms. Many patients are born as collodion babies (CBs). Later, the main symptoms are widespread scaling of the skin and varying degrees of erythema. ARCI includes a wide range of ichthyosis phenotypes. The main skin phenotypes are harlequin ichthyosis (HI, OMIM #242500), lamellar ichthyosis (LI, OMIM #242300), and congenital ichthyosiform erythroderma (CIE, OMIM #242100) [1].

The pathomechanisms and underlying genetic defects of ARCI have been elucidated recently. In addition, significant progress has been made toward understanding the molecular basis of human epidermal keratinization processes.

Since transglutaminase (TGase)-1 (*TGM1*) mutations were initially identified as the cause of LI in 1995 [2,3], several additional causal mutations have been detected in severe ARCI cases [4]. For instance, in 2005, we and other researchers reported loss-of-function mutations in the *ABCA12* gene in association with HI, the most severe type of ichthyosis [5,6].

To date, nine known genes are causally associated with ARCI in human patients [7], i.e., *ABCA12* [5,8–11], *TGM1* [2,3,12,13], the two lipoxygenase genes *ALOXE3* and *ALOX12B* [14,15], *NIPAL4* [16], *CYP4F22* [17,18], *PNPLA1* [19], *CERS3* [20,21], and *LIPN* [22] (Table 1). ARCI phenotypes exhibit a primary abnormality associated with barrier function in the stratum corneum as their underlying pathogenetic mechanism. The skin barrier of the stratum corneum has three major components, i.e., intercellular lipid layers, a cornified cell envelope, and keratin/filaggrin degradation products (Fig. 1).

In this review, we describe recent topics related to ARCI, highlighting the molecular mechanisms, causative genes, and clinical phenotypes of ARCI, and possible effective therapies. In addition, we briefly discuss mRNA analysis of hair samples, which is a minimally invasive method for mRNA analysis to aid in the genetic diagnosis of ARCI.

2. Causative ARCI genes and associated phenotypes

2.1. ABCA12

HI is a severe and often fatal congenital ichthyosis with an autosomal recessive inheritance pattern. It shows clinical features at birth including severe ectropion, eclabium, flattening of the ears, and large, thick, plate-like scales over the entire body. Neonatal death is not uncommon. HI is caused by severe functional defects in the keratinocyte lipid transporter ATP-binding cassette sub-family A member 12 (ABCA12) (Fig. 2). ABCA12 functional defects lead to the disruption of lamellar granule (LG) lipid transport in the upper epidermal keratinocytes.

Table 1
Causative genes and associated ARCI phenotypes.

Gene	Protein	Disease
ABCA12	ATP-binding cassette sub-family A member 12	HI, LI, CIE
TGM1	Transglutaminase-1	LI, CIE, SHCB, Acral SHCB, BSI
ALOXE3	Lipoxygenase-3	LI, CIE, SHCB
ALOX12B	12(R)-lipoxygenase	LI, CIE, SHCB
NIPAL4	Nipa-like domain-containing 4	LI, CIE
CYP4F22	Cytochrome P450, family F polypeptide 2 homolog of leukotriene B4-omega-hydroxylase	LI
PNPLA1	Patatin-like phospholipase domain protein 1	LI
CERS3	Ceramide synthase 3	LI
LIPN	Lipase N	LI

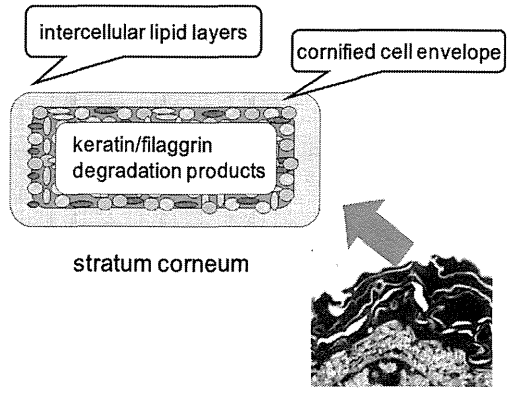

Fig. 1. Three major components of the stratum corneum that form the skin barrier. The major components are intercellular lipid layers, a cornified cell envelope, and keratin/filaggrin degradation products.

Mutations in *ABCA12* are known to cause not only HI, but also CIE and LI. In a review of the literature on *ABCA12* mutations in patients with ARCI, we identified 56 known *ABCA12* mutations in 66 globally distributed, unrelated families, including 48 HI, 10 LI, and 8 CIE families [23]. Of the 56 mutations, 36% are nonsense, 25% are missense, 20% are small deletion, 11% are splice-site, 5% are large-deletion, and 4% are insertion mutations. At least 62.5% of all reported mutations are predicted to result in truncated proteins. There is no obvious mutation hot spot in *ABCA12*, although mutations underlying the LI phenotype are clustered in the domain containing the first ATP-binding cassette.

Recent advances in HI research have revealed that high frequencies of HI can be improved with intensive neonatal care. Milstone and Choate [24] reported that the early introduction of overall intensive therapy might have contributed to better outcomes observed in HI babies who were given oral retinoids. Indeed, the outcomes of HI babies have recently improved in Japan. In a study of HI cases in Japan [25], we obtained clinical data for 16 HI patients between 2005 and 2010. Among them, there were 13 survivors (81.3%) and 3 deceased subjects (18.7%). Overall, we inferred that intensive neonatal care and, probably, early intervention using oral retinoids, have improved HI outcomes.

Recently, we identified the promoter region of *ABCA12* and located the essential elements therein; thus, the information necessary for genetic diagnostic screening for *ABCA12* mutations that cause congenital ichthyosis is available [26]. Specifically, we showed that ABCA12 expression in differentiating cultured human keratinocytes is critically dependent on a palindromic motif that resides in the region from −2084 to −2078 relative to the transcription start site (Fig. 3) [26].

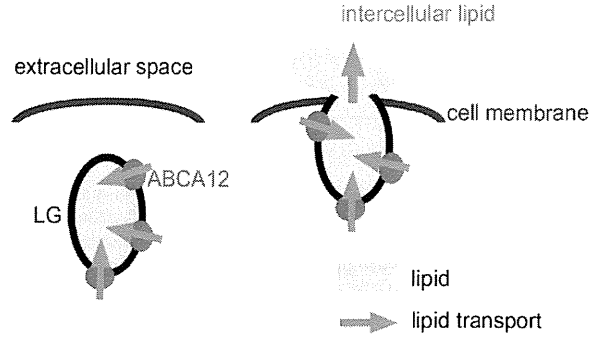

Fig. 2. Function of ABCA12. ABCA12 is a keratinocyte transmembrane lipid transporter protein associated with the transport of lipids by lamellar granules to the apical surface of granular layer keratinocytes. LG, lamellar granule.

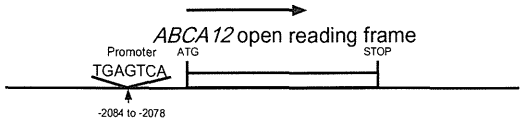

Fig. 3. Scheme of the *ABCA12* gene promoter. A palindromic motif (tgagtca) at −22084 to −22078 is essential for the promoter function of *ABCA12*.

As mentioned above, HI patients sometimes die during the perinatal period. However, most patients who survive beyond the neonatal period exhibit gradual phenotypic improvement from a few weeks to several months after birth [25]. To determine the mechanisms of phenotypic recovery, we investigated grafted skin and keratinocytes from *Abca12*-deficient (*Abca12*$^{-/-}$) mice [27]. We observed remarkable improvements for all if the abnormalities in the model mice with *Abca12*$^{-/-}$ skin grafts kept in a dry environment. The increased trans-epidermal water loss due to barrier defect was dramatically mitigated in the grafted *Abca12*$^{-/-}$ skin kept in a dry environment. An abnormal ceramide distribution, defective expression of differentiation-specific proteins, and profilaggrin/filaggrin conversion were observed in the primary culture of *Abca12*$^{-/-}$ keratinocytes, but these abnormalities were resolved in ten-passage sub-cultured *Abca12*$^{-/-}$ keratinocytes. These findings suggest that *Abca12*$^{-/-}$ epidermal keratinocytes restore normal differentiation during maturation. The precise mechanisms of this restoration of keratinocyte differentiation remain to be clarified, but the mitigation of keratinocyte differentiation defects may facilitate the development of novel therapies for the ichthyosis phenotype.

Cottle et al. [28] observed a pro-inflammatory signature characterized by chemokine upregulation in embryonic skin on *Abca12*-deficient mice. To examine the contribution of inflammation to disease development, they overexpressed interleukin-37b, an immunosuppressive interleukin, to globally suppress fetal inflammation. Considerable improvements in keratinocyte differentiation were observed in *Abca12*-deficient mice [28]. This result suggests a possible therapy for human ARCI involving *ABCA12* mutations.

2.2. TGM1

The cornified cell envelope on the inner surface of the cell membrane is essential for skin barrier function [29]. TGases in the epidermis are thought to be responsible, at least in part, for the assembly of cornified cell envelope precursor proteins, including involucrin, small proline-rich proteins, and loricrin, to form the cornified cell envelope [30]. The membrane-associated TGase-1 is the major TGase subtype expressed in the epidermis. Since the identification of TGase-1 (*TGM1*) mutations in a number of families with LI in 1995 [2,3], additional *TGM1* mutations associated with LI have been reported [12]. *TGM1* mutations have also been reported to underlie the CIE phenotype [31].

TGM1 mutations are not always related to severe phenotypes of ARCI. They sometimes cause very mild LI or self-healing collodion baby (SHCB), also termed self-improving collodion baby [32]. SHCB refers to a baby who is born as a collodion baby, but improves spontaneously. We recently identified missense mutations in the β-barrel domains of TGase-1 in arginine residues in very mild LI (Fig. 4A) and SHCB cases [12,33]. In LI, the majority of causative *TGM1* mutations have been identified in the central core domain or upstream of it. In contrast, mutations in β-barrel domains in the carboxyl-terminus of the gene are rarely found [7]. Several authors suggest that β-barrel domains increase TGase-1 activity, but are not essential for the basic function of the enzyme [8,9]. Clinically, other minor ARCI variants can be distinguished, e.g., bathing suit ichthyosis has been attributed to particular *TGM1* mutations that render the enzyme sensitive to ambient temperature. In acral SHCB, a very rare type, the collodion membrane is strictly localized to the extremities at birth and eventually resolves. This phenotype is also a result of *TGM1* mutations (Table 1) [1].

Recently, Aufenvenne et al. [34] have developed the basis for an enzyme-replacement therapy for individuals suffering from TGase1-deficient ARCI. They demonstrated that a topical approach using a formulation of liposomal-encapsulated recombinant human TGase-1 is suitable for restoring TGase-1 activity in the upper stratified layers of the epidermis to reconstitute epidermal integrity and barrier function in a mouse model. This result suggests a possible therapy for ARCI due to *TGM1* mutations.

2.3. ALOXE3 and ALOX12B

Mutations in two lipoxygenase genes, *ALOXE3* and *ALOX12B*, coding lipoxygenase-3 (eLOX-3) and 12(R)-lipoxygenase (12R-LOX), respectively, were reported to underlie ARCI in 2002 [14]. Oxygenation of the linoleate moiety of ceramides

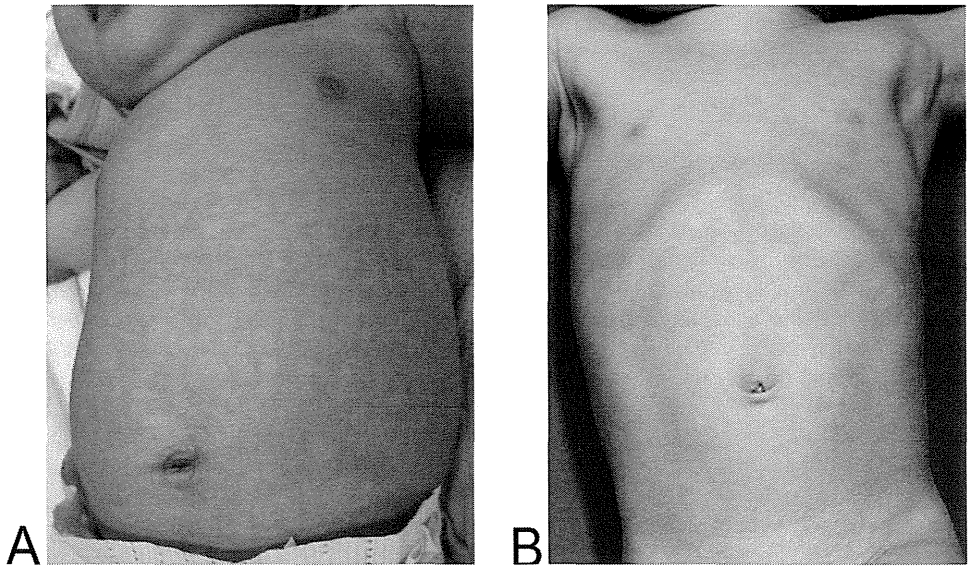

Fig. 4. Clinical features of mild LI with *TGM1* mutations and LI with *CYP4F22* mutations. Scales with slight partial erythema on the trunk of the patient are shown. The figures 4A and B are from Sugiura et al. [12] and Sugiura et al. [18], respectively. Scales on trunk of the patient (A) and scales with slight partial erythema on the trunk of the patient (B) are shown.

catalyzed by 12R-LOX/eLOX-3 constitutes an indispensable step for the covalent linkage of ω-hydroxyl ceramides to proteins of the cornified cell envelope and subsequently for the formation of the corneocyte lipid envelope. Furthermore, analysis of *Aloxe3*-knockout mice revealed a function of epidermal lipoxygenase-3 as a hepoxilin synthase and its pivotal role in barrier formation [35]. ARCI phenotypes caused by *ALOXE3* mutations are categorized as CIE, LI, or SHCB. LI patients with *ALOXE3* mutations have been identified in Europe, North Africa, the Middle East, and South Asia, and, recently, an LI patient with *ALOXE3* mutations was also reported in East Asia [15].

2.4. NIPAL4

Defects of NIPA-like domain-containing 4 (NIPAL4), encoded by NIPAL4, have also been linked to cases of LI or CIE phenotypes [16]. NIPAL4 has several transmembrane domains and belongs to a new family of proteins and its function is unknown. Li et al. [16] recently suggested that fatty acid transport protein 4 (FATP4), NIPAL4, and TGase-1 interact in lipid processing, which is essential for maintaining epidermal barrier function. It is also hypothesized that NIPAL4 serves as an Mg^{2+} transporter for FATP4 in this process [16]. FATP4 belongs to a family of six transmembrane proteins that facilitate long- and very long-chain fatty acid uptake [36]. FATP4 is expressed in several tissue types, including the skin. Mutations in human *SLC27A4*, which encodes FATP4, cause ichthyosis prematurity syndrome, characterized by a thick desquamating epidermis and premature birth [37].

2.5. CYP4F22

Mutations in *CYP4F22* have been identified as causative genetic defects in LI type 3 (OMIM #604777) [17]. *CYP4F22* encodes a cytochrome P450, family F polypeptide 2 homolog of leukotriene B4-omega-hydroxylase (CYP4F22). CYP4F22 is thought to be an orphan CYP. Its function has not yet been clarified, but CYP4F22 is highly expressed at the location and time corresponding to the onset of keratinization during skin development [38]. Patients with LI caused by *CYP4F22* mutations are very rare; only three reports cases have been reported in the literature. These reports describe homozygous mutations from consanguineous families in the Mediterranean region and Japan (Fig. 4B) [17,18]. Recently, we suggested possible genotype/phenotype correlations for *CYP4F22* mutations, i.e., a patient harboring one or two truncating CYP4F22 mutations affecting substrate-binding regions may be born as a collodion baby [18].

2.6. PNPLA1

PNPLA1 was identified as a novel ARCI-causing gene in 2012 [19]. It encodes patatin-like phospholipase domain protein 1 (PNPLA1). All affected individuals with *PNPLA1* mutations are born as CBs and the impairment seems to be congenital and severe at birth. The function of PNPLA1 is unknown, although it appears to play a key role in lipid synthesis and metabolism during epidermal barrier formation, which is of prime importance in the keratinization process and terminal differentiation of keratinocytes.

2.7. CERS3

CERS3, which encodes ceramide synthase 3 (CERS3), was identified as a causative gene of ARCI in 2013 [20,21]. Functional analysis of a skin sample and in vitro differentiated keratinocytes from a patient demonstrated that mutated CERS3 impairs the synthesis of ceramides with very long-chain acyl moieties [21].

2.8. LIPN

In affected members of a consanguineous Arab pedigree with a late-onset LI (#OMIN 613943), Israeli et al. [22] identified *LIPN* as a causative gene. *LIPN* encodes lipase N (LIPN). Although the function of LIPN has not been elucidated, it is thought to play a role in the differentiation of human keratinocytes [22].

3. Challenges related to the precise diagnosis of ARCI even with genetic tools

Dorfman–Chanarin syndrome (DCS) is a rare autosomal recessive form of congenital ichthyosis, characterized by the presence of intracellular lipid droplets in multiple organs [39,40] (OMIM #275630). Liver dysfunction and mental retardation are major extra-cutaneous manifestations of DCS [41,42]. DCS patients often have mutations in *ABHD5* (also termed as *CGI-58*), which encodes α/β hydrolase domain-containing 5 (ABHD5)/comparative gene identification 58 (CGI-58), an activator of adipose triglyceride lipase. ABHD5 deficiency leads to triglyceride accumulation [43,44]. We recently reported a case of DCS without mental retardation, caused by a homozygous *ABDH5* splicing site mutation [45]. We suggested that the *ABHD5* splicing site mutation, which results in the skipping of the entire exon 6, is associated with a DCS phenotype lacking mental retardation [45].

Takeichi et al. [46] have recently demonstrated the impact of next-generation sequencing technologies on clinical genetics in the dermatology field. Indeed, next-generation sequencing can reveal two autosomal recessive disorders in a single family. For example, in a patient showing an ARCI phenotype, mutations in both *ST14* and *POMT1*, which encode suppression of tumorigenicity 14 and *O*-mannosyltransferase, respectively, were detected by next-generation sequencing [47]. *ST14* is a causative gene for ARCI11 (OMIM #602400), known as ARCI with hypotrichosis, and follicular atrophoderma with hypotrichosis and hypohidrosis. *POMT1* is a causative gene for Walker–Warburg syndrome, a rare autosomal recessive disorder with developmental malformations.

4. mRNA analysis of hair samples to aid in genetic diagnosis

We hypothesized that mRNA expression in hair follicle epithelial cells is analogous to that of interfollicular epidermal cells. Accordingly, we developed an innovative method for skin epithelial mRNA analysis using RNA extracted from plucked hair samples to analyze mRNA expression in epithelial cells (keratinocytes). We confirmed that *ABCA12* mRNA expression in cutaneous epithelial cells can be analyzed using our method. That is, total RNA extracted from plucked hairs was successfully analyzed without performing invasive skin biopsies, to our knowledge, for the first time (Fig. 5) [8]. Total RNA was extracted from hair roots and cDNAs were obtained by reverse transcription-PCR. In an HI patient, the expression of *ABCA12* mRNA was evaluated by quantitative PCR using the cDNAs to estimate mRNA decay. Sequencing of the cDNA extracted from hair samples also demonstrated the aberrant splicing patterns due to splice-site mutations [8]. We recently applied our method using plucked hairs to analyze mRNA expression of other genes, including *IL36RN*, *ABHD5*, and *TRPS1*, in cutaneous epithelial cells [45,48–50]. Our method for the analysis of mRNA expression in epithelial cells (keratinocytes) using plucked hair samples can be applied to the diagnosis of not only keratinization disorders, but also many other genetic diseases in the dermatology field.

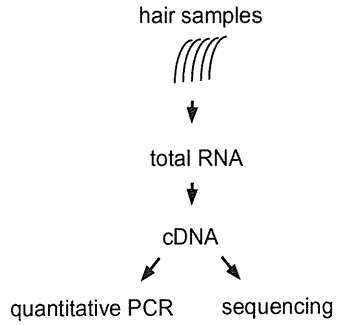

Fig. 5. Flowchart for the mRNA analysis of hair samples to aid in genetic diagnosis.

5. Concluding remarks

Knowledge of the molecular genetics and pathogenesis of ichthyosis has advanced dramatically. A genetic diagnosis method utilizing next-generation sequencing and analysis of mRNA using hair samples has been developed. In addition, the results of studies using disease models have suggested possible therapies for ARCI due to *ABCA12* or *TGM1* mutations. An increasing number of intensive studies on ARCI and causative molecules will promote efficient therapeutic methods for ARCI patients.

Funding

None.

Acknowledgements

This study was supported in part by a Grant-in-Aid for Scientific Research (A) 23249058 (to M.A.) from the Ministry of Education, Culture, Sports, Science, and Technology of Japan, and by the grant H26-itaku (nan)-ippan-027 (to K.S.) from the Ministry of Health, Labour, and Welfare (Research on Measures for Intractable Disease), Japan.

References

[1] Oji V, Tadini G, Akiyama M, Blanchet Bardon C, Bodemer C, Bourrat E, et al. Revised nomenclature and classification of inherited ichthyoses: results of the First Ichthyosis Consensus Conference in Soreze 2009. J Am Acad Dermatol 2010;63:607–41.
[2] Russell LJ, DiGiovanna JJ, Rogers GR, Steinert PM, Hashem N, Compton JG, et al. Mutations in the gene for transglutaminase 1 in autosomal recessive lamellar ichthyosis. Nat Genet 1995;9:279–83.
[3] Huber M, Rettler I, Bernasconi K, Frenk E, Lavrijsen SP, Ponec M, et al. Mutations of keratinocyte transglutaminase in lamellar ichthyosis. Science 1995;267:525–8.
[4] Akiyama M. Harlequin ichthyosis and other autosomal recessive congenital ichthyoses: the underlying genetic defects and pathomechanisms. J Dermatol Sci 2006;42:83–9.
[5] Akiyama M, Sugiyama-Nakagiri Y, Sakai K, McMillan JR, Goto M, Arita K, et al. Mutations in lipid transporter ABCA12 in harlequin ichthyosis and functional recovery by corrective gene transfer. J Clin Invest 2005;115:1777–84.
[6] Kelsell DP, Norgett EE, Unsworth H, Teh MT, Cullup T, Mein CA, et al. Mutations in ABCA12 underlie the severe congenital skin disease harlequin ichthyosis. Am J Hum Genet 2005;76:794–803.
[7] Numata S, Teye K, Krol RP, Karashima T, Fukuda S, Matsuda M, et al. Mutation study for 9 genes in 23 unrelated patients with autosomal recessive congenital ichthyosis in Japan and Malaysia. J Dermatol Sci 2015.
[8] Takeichi T, Sugiura K, Matsuda K, Kono M, Akiyama M. Novel ABCA12 splice site deletion mutation and ABCA12 mRNA analysis of pulled hair samples in harlequin ichthyosis. J Dermatol Sci 2013;69:259–61.
[9] Shimizu Y, Sugiura K, Aoyama Y, Ogawa Y, Hitomi K, Iwatsuki K, et al. Novel ABCA12 missense mutation p.Phe2144Ser underlies congenital ichthyosiform erythroderma. J Dermatol 2013;40:581–2.
[10] Akiyama M, Sakai K, Hatamochi A, Yamazaki S, McMillan JR, Shimizu H. Novel compound heterozygous nonsense and missense ABCA12 mutations lead to nonbullous congenital ichthyosiform erythroderma. Br J Dermatol 2008;158:864–7.
[11] Lefevre C, Audebert S, Jobard F, Bouadjar B, Lakhdar H, Boughdene-Stambouli O, et al. Mutations in the transporter ABCA12 are associated with lamellar ichthyosis type 2. Hum Mol Genet 2003;12:2369–78.
[12] Sugiura K, Suga Y, Akiyama M. Very mild lamellar ichthyosis with compound heterozygous TGM1 mutations including the novel missense mutation p.Leu693Phe. J Dermatol Sci 2013;72:197–9.
[13] Sugiura K. Unfolded protein response in keratinocytes: impact on normal and abnormal keratinization. J Dermatol Sci 2013;69:181–6.
[14] Jobard F, Lefevre C, Karaduman A, Blanchet-Bardon C, Emre S, Weissenbach J, et al. Lipoxygenase-3 (ALOXE3) and 12(R)-lipoxygenase (ALOX12B) are mutated in non-bullous congenital ichthyosiform erythroderma (NCIE) linked to chromosome 17p13.1. Hum Mol Genet 2002;11:107–13.
[15] Sugiura K, Akiyama M. Lamellar ichthyosis caused by a previously unreported homozygous ALOXE3 Mutation in East Asia. Acta Derm Venereol 2014.
[16] Li H, Vahlquist A, Torma H. Interactions between FATP4 and ichthyin in epidermal lipid processing may provide clues to the pathogenesis of autosomal recessive congenital ichthyosis. J Dermatol Sci 2013;69:195–201.
[17] Lefevre C, Bouadjar B, Ferrand V, Tadini G, Megarbane A, Lathrop M, et al. Mutations in a new cytochrome P450 gene in lamellar ichthyosis type 3. Hum Mol Genet 2006;15:767–76.
[18] Sugiura K, Takeichi T, Tanahashi K, Ito Y, Kosho T, Saida K, et al. Lamellar ichthyosis in a collodion baby caused by CYP4F22 mutations in a non-consanguineous family outside the Mediterranean. J Dermatol Sci 2013;72:193–5.
[19] Grall A, Guaguere E, Planchais S, Grond S, Bourrat E, Hausser I, et al. PNPLA1 mutations cause autosomal recessive congenital ichthyosis in golden retriever dogs and humans. Nat Genet 2012;44:140–7.
[20] Radner FP, Marrakchi S, Kirchmeier P, Kim GJ, Ribierre F, Kamoun B, et al. Mutations in CERS3 cause autosomal recessive congenital ichthyosis in humans. PLoS Genet 2013;9:e1003536.
[21] Eckl KM, Tidhar R, Thiele H, Oji V, Hausser I, Brodesser S, et al. Impaired epidermal ceramide synthesis causes autosomal recessive congenital ichthyosis and reveals the importance of ceramide acyl chain length. J Invest Dermatol 2013;133:2202–11.
[22] Israeli S, Khamaysi Z, Fuchs-Telem D, Nousbeck J, Bergman R, Sarig O, et al. A mutation in LIPN, encoding epidermal lipase N, causes a late-onset form of autosomal-recessive congenital ichthyosis. Am J Hum Genet 2011;88:482–7.
[23] Akiyama M. ABCA12 mutations and autosomal recessive congenital ichthyosis: a review of genotype/phenotype correlations and of pathogenetic concepts. Hum Mutat 2010;31:1090–6.
[24] Milstone LM, Choate KA. Improving outcomes for harlequin ichthyosis. J Am Acad Dermatol 2013;69:808–9.
[25] Shibata A, Ogawa Y, Sugiura K, Muro Y, Abe R, Suzuki T, et al. High survival rate of harlequin ichthyosis in Japan. J Am Acad Dermatol 2014;70:387–8.
[26] Shimizu Y, Ogawa Y, Sugiura K, Takeda J, Sakai-Sawada K, Yanagi T, et al. A palindromic motif in the −2084 to −2078 upstream region is essential for ABCA12 promoter function in cultured human keratinocytes. Sci Rep 2014;4:6737.
[27] Yanagi T, Akiyama M, Nishihara H, Ishikawa J, Sakai K, Miyamura Y, et al. Self-improvement of keratinocyte differentiation defects during skin maturation in ABCA12-deficient harlequin ichthyosis model mice. Am J Pathol 2010;177:106–18.
[28] Cottle DL, Ursino GM, Ip SC, Jones LK, Ditommaso T, Hacking DF, et al. Fetal inhibition of inflammation improves disease phenotypes in harlequin ichthyosis. Hum Mol Genet 2015;24:436–49.
[29] Akiyama M, Shimizu H. An update on molecular aspects of the non-syndromic ichthyoses. Exp Dermatol 2008;17:373–82.
[30] Kim IG, McBride OW, Wang M, Kim SY, Idler WW, Steinert PM. Structure and organization of the human transglutaminase 1 gene. J Biol Chem 1992;267:7710–7.
[31] Akiyama M, Takizawa Y, Kokaji T, Shimizu H. Novel mutations of TGM1 in a child with congenital ichthyosiform erythroderma. Br J Dermatol 2001;144:401–7.
[32] Vahlquist A, Bygum A, Ganemo A, Virtanen M, Hellstrom-Pigg M, Strauss G, et al. Genotypic and clinical spectrum of self-improving collodion ichthyosis: ALOX12B, ALOXE3, and TGM1 mutations in Scandinavian patients. J Invest Dermatol 2010;130:438–43.
[33] Tanahashi K, Sugiura K, Asagoe K, Aoyama Y, Iwatsuki K, Akiyama M. Novel TGM1 missense mutation p.Arg727Gln in a case of self-healing collodion baby. Acta Derm Venereol 2014;94:589–90.
[34] Aufenvenne K, Larcher F, Hausser I, Duarte B, Oji V, Nikolenko H, et al. Topical enzyme-replacement therapy restores transglutaminase 1 activity and corrects architecture of transglutaminase-1-deficient skin grafts. Am J Hum Genet 2013;93:620–30.
[35] Krieg P, Rosenberger S, de Juanes S, Latzko S, Hou J, Dick A, et al. Aloxe3 knockout mice reveal a function of epidermal lipoxygenase-3 as hepoxilin synthase and its pivotal role in barrier formation. J Invest Dermatol 2013;133:172–80.
[36] Schaffer JE, Lodish HF. Expression cloning and characterization of a novel adipocyte long chain fatty acid transport protein. Cell 1994;79:427–36.
[37] Klar J, Schweiger M, Zimmerman R, Zechner R, Li H, Torma H, et al. Mutations in the fatty acid transport protein 4 gene cause the ichthyosis prematurity syndrome. Am J Hum Genet 2009;85:248–53.